



1

2

3

4

5 **High-resolution regional emission inventory contributes to**
6 **the evaluation of policy effectiveness: A case study in Jiangsu**
7 **province, China**

8

9 Chen Gu¹, Lei Zhang^{1,2}, Zidie Xu¹, Sijia Xia³, Yutong Wang¹, Li Li³, Zeren Wang¹,
10 Qiuyue Zhao³, Hanying Wang¹, Yu Zhao^{1,2*}

11

12 ¹ State Key Laboratory of Pollution Control and Resource Reuse and School of the
13 Environment, Nanjing University, 163 Xianlin Rd., Nanjing, Jiangsu 210023, China

14 ² Collaborative Innovation Center of Atmospheric Environment and Equipment
15 Technology, CICAET, Nanjing, Jiangsu 210044, China

16 ³ Jiangsu Key Laboratory of Environmental Engineering, Jiangsu Provincial Academy
17 of Environmental Sciences, Nanjing, Jiangsu 210036, China

18

19 *Corresponding author: Yu Zhao

20 Phone: 86-25-89680650; email: yuzhao@nju.edu.cn

21

22

23

24

25



26 **Abstract**

27 China has been conducting a series of actions on air quality improvement for the past
28 decades, and air pollutant emissions have been changing swiftly across the country.
29 Province is an important administrative unit for air quality management, thus reliable
30 provincial-level emission inventory for multiple years is essential for detecting the
31 varying sources of pollution and evaluating the effectiveness of emission controls. In
32 this study, we selected Jiangsu, one of the most developed provinces in China, and
33 developed the high-resolution emission inventory of nine species for 2015-2019, with
34 improved methodologies for different emission sectors, best available facility-level
35 information on individual sources, and real-world emission measurements. Resulting
36 from implementation of strict emission control measures, the anthropogenic emissions
37 were estimated to have declined 53%, 20%, 7%, 2%, 10%, 21%, 16%, 6% and 18%
38 for SO₂, NO_x, CO, NMVOCs, NH₃, PM₁₀, PM_{2.5}, BC, and OC from 2015 to 2019,
39 respectively. Larger abatement of SO₂, NO_x and PM_{2.5} emissions were detected for
40 the more developed southern Jiangsu. Since 2016, the ratio of biogenic volatile
41 organic compounds (BVOCs) to anthropogenic volatile organic compounds (AVOCs)
42 exceeded 50% in July, indicating the importance of biogenic sources on summer O₃
43 formation. Our estimates in annual emissions of NO_x, NMVOCs, and NH₃ were
44 generally smaller than the national emission inventory MEIC, but larger for primary
45 particles. The discrepancies between studies resulted mainly from different methods
46 of emission estimation (e.g., the procedure-based approach for AVOCs emissions
47 from key industries used in this work) and inconsistent information of emission
48 source operation (e.g., the penetrations and removal efficiencies of air pollution
49 control devices). Regarding the different periods, more reduction of SO₂ emissions
50 was found between 2015 and 2017, but NO_x, AVOCs and PM_{2.5} between 2017 and
51 2019. Among the selected 13 major measures, the ultra-low emission retrofit on
52 power sector was the most important contributor to the reduced SO₂ and NO_x
53 emissions (accounting for 38% and 43% of the emission abatement, respectively) for
54 2015-2017, but its effect became very limited afterwards as the retrofit had been



55 commonly completed by 2017. Instead, extensive management of coal-fired boilers
56 and upgradation and renovation of non-electrical industry were the most important
57 measures for 2017-2019, accounted collectively for 61%, 49% and 57% reduction of
58 SO₂, NO_x and PM_{2.5}, respectively. Controls on key industrial sectors maintained the
59 most effective for AVOCs reduction for the two periods, while measures on other
60 sources (transportation and solvent replacement) became increasingly important for
61 more recent years. Our provincial emission inventory was demonstrated to be
62 supportive for high-resolution air quality modeling for multiple years. Through
63 scenario setting and modeling, worsened meteorological conditions were found from
64 2015 to 2019 for PM_{2.5} and O₃ pollution alleviation. However, the efforts on emission
65 controls were identified to largely overcome the negative influence of meteorological
66 variation. The changed anthropogenic emissions were estimated to contribute 4.3 and
67 5.5 μg·m⁻³ of PM_{2.5} concentration reduction for 2015-2017 and 2017-2019,
68 respectively. While elevated O₃ by 4.9 μg·m⁻³ for 2015-2017, the changing emissions
69 led to 3.1 μg·m⁻³ of reduction for 2017-2019, partly (not fully though) offsetting the
70 meteorology-driven growth. The analysis justified the validity of local emission
71 control efforts on air quality improvement, and provided scientific basis to formulate
72 air pollution prevention and control policies for other developed regions in China and
73 worldwide.

74 **1. Introduction**

75 Severe air pollution is of great concern for fast industrialized countries like China,
76 especially in economically developed regions where an overlap of serious pollution
77 levels and dense populations has resulted in high exposure and adverse health
78 outcomes (Klimont et al., 2013; Hoesly et al., 2018). Emission inventory, which
79 contains complete information on magnitude, spatial pattern, and temporal change of
80 air pollutant emissions by sector, is essential for identifying the sources of air
81 pollution and effectiveness of emission controls on air quality through numerical
82 modeling (Zhao et al., 2013). Improving the understanding of emission behaviors and



83 reducing the uncertainty of emission estimates have always been the main focus of
84 emission inventory studies, given the big variety of source categories, fast changing
85 mix of manufacturing and emission control technologies, and insufficient
86 measurements of real-world emissions. At the global and continental scales, emission
87 inventories have been developed by combining available information of large point
88 sources and improved surrogate statistics for area sources, e.g., Emissions Database
89 for Global Atmospheric Research (EDGAR, <https://edgar.jrc.ec.europa.eu/>, Crippa et
90 al., 2020) and Regional Emission Inventory in Asia (REAS,
91 <https://www.nies.go.jp/REAS/>, Kurokawa et al., 2020). As the largest developing
92 country in the world, China has been proven to contribute significantly to global
93 emissions (Klimont et al., 2013; Huang et al., 2014; Wiedinmyer et al., 2014;
94 Miyazaki et al., 2017).

95 Along with the gradually improved methodology and increasingly availability of
96 emission source and field measurement data, the applicability and reliability of recent
97 Chinese emission inventories (e.g., the Multi-resolution Emission Inventory for China,
98 MEIC, Zheng et al., 2018) have been significantly improved compared to the earlier
99 large-scale studies for Asia or the world. When the research focus switches to smaller
100 provincial and city scales, the uncertainty of national emission inventory may increase
101 attributed mainly to the insufficient information on detailed emission sources,
102 particularly for medium/small size stationary and area sources. Certain “proxies”
103 including population and economic densities were commonly applied to downscale
104 the emissions from coarser to finer horizontal resolution, based on the assumption that
105 those proxies were strongly associated with emission intensity. Such “coupling effect”,
106 however, has been demonstrated to be largely weakened, leading to great uncertainty
107 in emission estimation and consequently enhanced bias in air quality modeling (Zhou
108 et al., 2017; Zheng et al., 2017). For the urgent demand for preventing regional air
109 pollution and relevant health damage, therefore, development of high-resolution
110 emission inventories has been getting increasingly essential, especially in regions with
111 developed industry, large population and complex emission sources (Zheng et al.,
112 2009; Shen et al., 2017; Zhao et al., 2018). With increased proportion of point sources



113 and more complete facility-based information, the improved emission inventory could
114 largely reduce the arbitrary use of proxy-based downscaling technique and thereby the
115 uncertainty of the emission estimates (Zhao et al., 2015; Zheng et al., 2021).
116 For the past decade, China has been conducting a series of actions to tackle the
117 serious air pollution problem. With the mitigation of severe fine particulate matter
118 (PM_{2.5}) pollution set as a priority from 2013 to 2017, the National Action Plan on Air
119 Pollution Control and Prevention (NAPAPCP, State Council of the People's Republic
120 of China (SCC), 2013) pushed stringent end-of-pipe emission controls (e.g., the
121 “ultra-low” emission control for power sector) and retirement of small and
122 energy-inefficient factories (Zhang et al., 2019a; 2019b; Zheng et al., 2018). On top of
123 that, China announced the “Three-Year Action Plan to Fight Air Pollution”
124 (TYAPFAP) to further reduce PM_{2.5} and ozone (O₃) levels for 2018-2020 (SCC, 2018).
125 Substantially enhanced measures have been required for reducing industrial (e.g.,
126 application of “ultra-low” emission control for selected non-electrical industries) and
127 residential emissions (e.g., promotion of advanced stoves and clean coal during
128 heating seasons). Those measures have significantly changed the air pollutant
129 emissions and thereby air quality over the country. Studies have been conducted to
130 assess the contribution of the nation actions to the improvement of air quality, based
131 usually on the national emission inventory. For example, Zhang et al. (2019a)
132 estimated a nationwide 30-40% reduction in PM_{2.5} concentration attributed to
133 NAPAPCP from 2013 to 2017.
134 Province is an important administrative unit for air quality management. Given the
135 heterogeneous economical and energy structures as well as atmospheric conditions,
136 there are usually big diversities in the strategies and actions of reducing regional air
137 pollution adopted by the local governments, leading to various progresses of emission
138 and air quality changes (Liu et al., 2022; Wang et al., 2021a). Limited by incomplete
139 or inconsecutive information on emission sources and lack of on-time emission
140 measurements, however, there were relatively few studies on provincial-level
141 emission inventories for multiple years. Studies based on the national emission
142 inventories would be less supportive for policy makers to formulate the emission



143 control measures and to evaluate their effectiveness on emission reduction and air
144 quality improvement (An et al., 2021; Huang et al., 2021). Contrary to NAPAPCP that
145 has been increasingly noticed, moreover, few analyses have been conducted for
146 TYAPFAP after 2017 due partly to lack of most recent emission data, preventing
147 comparison and comprehensive understanding of the effectiveness of emission
148 controls for the two phases. Jiangsu Province, located on the northeast coast of the
149 Yangtze River Delta region (YRD), is one of China's most industrial developed and
150 heavy-polluted regions. It comprised 10.1% of the gross domestic product (GDP) in
151 mainland China (ranking the second place in the country), and 6.4%, 11.3% and 11.4%
152 of national cement, pig iron and crude steel production in 2020, respectively (National
153 Bureau of Statistics of China, 2021). MEIC indicated the emissions per unit area of
154 anthropogenic sulfur dioxide (SO₂), nitrogen oxides (NO_x), non-methane volatile
155 organic compounds (NMVOCs), PM_{2.5}, and ammonia (NH₃) in Jiangsu were 2.8, 6.5,
156 7.0, 4.5 and 4.8 times of the national average in 2017, respectively. Resulting from the
157 implementation of air pollution prevention measures, PM_{2.5} pollution in Jiangsu has
158 been significantly alleviated since 2013, while the great changes in emissions due to
159 varying energy use and industry and transportation development have made it become
160 the province with the highest O₃ concentration and the fastest growth rate of O₃ in
161 YRD for recent years (Zheng et al., 2016; Wang et al., 2017; Zhang et al., 2017a;
162 Zhou et al., 2017).

163 In this study, therefore, we took Jiangsu as an example to demonstrate the
164 development of high-resolution emission inventory and its application on evaluating
165 the effectiveness of emission control actions. We integrated the methodological
166 improvements on regional emission inventory by our previous studies (Zhou et al.,
167 2017; Zhao et al., 2017; 2020; Wu et al., 2022; Zhang et al., 2019b; Zhang et al., 2020;
168 2021b), and compiled and incorporated best available facility-level information and
169 real-world emission measurements (see details in the methodology and data section).
170 A provincial-level emission inventory for 2015-2019 was then thoroughly developed
171 for nine gaseous and particulate species (SO₂, NO_x, NMVOCs, carbon dioxide (CO),
172 inhalable particulate matter (PM₁₀), PM_{2.5}, NH₃, black carbon (BC), and organic



173 carbon (OC)). The difference between our emission inventory and others, as well as
174 its main causes, was carefully explored. Using a measure-specific integrated
175 evaluation approach, we further identified the drivers of emission changes of SO₂,
176 NO_x, PM_{2.5} and anthropogenic volatile organic compounds (AVOCs), with an
177 emphasis on the impacts of 13 major control measures summarized from NAPAPCP
178 and TYAPFAP. Finally, air quality modeling was applied to assess the reliability of
179 our emission inventory and to quantify the contribution of emission controls to the
180 changing PM_{2.5} and O₃ concentrations for 2015-2017 within NAPAPCP and
181 2017-2019 within TYAPFAP, and the differentiated impacts of emission controls on
182 air quality were revealed for the two phases.

183 **2. Methodology and data**

184 **2.1 Emission estimation**

185 **2.1.1 Emission source classification**

186 We applied a four-level framework of emission source categories for Jiangsu emission
187 inventory, based on a thorough investigation on the energy and industrial structures in
188 the province. The framework included six first-level categories this study, covering all
189 the social and economic sectors in Jiangsu: power sector, industry, transportation,
190 agriculture, residential, and biogenic source (for NMVOCs only). Moreover, the
191 framework contained fifty-five second-level categories based on facility/equipment
192 types and economical subsectors (see details in Table S1 in the Supplement), 240
193 third-level categories classified mainly by fuel, product, and material types, and a total
194 of 870 fourth-level categories including sources by combustion, manufacturing and
195 emission control technologies of emission facilities.

196 Compared to guidelines for development of national emission inventories (He et al.,
197 2018), forty-two new categories (third-level) were added in this study, contained
198 mainly in the second-level categories including metal products and the mechanical
199 equipment manufacturing industries, non-industrial solvent usage from ship fittings



200 and repairs, household appliances, and housing retrofitting emissions. Those
201 categories were identified as important sources of NMVOCs emissions in Jiangsu. In
202 particular, ship coating emissions, coming mainly from solvent usage during spraying,
203 cleaning and gluing in a wide range of procedures, could account for nearly 20% of
204 the solvent use emissions in the YRD region (Mo et al., 2021). Therefore, the updated
205 framework provided a more complete coverage of source categories, thus was able to
206 considerably reduce the bias of emission estimation due to missing potentially
207 important emitters.

208 **2.1.2 Emission estimation methods**

209 We applied the “bottom-up” methodology (i.e., the emissions were calculated at the
210 finest source level (e.g., facility level if data allowed) and then aggregated to upper
211 categories/regions) to develop the high-resolution emission inventory for Jiangsu (and
212 its 13 cities, as shown in Figure S1 in the Supplement) 2015-2019. As mentioned in
213 Introduction, we have conducted a series of studies and made substantial
214 improvements on the methodology of regional emission inventory development by
215 source category or species, compared to the ones at larger spatial scales. Here we
216 integrated those improvements as briefly described below, and additional further
217 details can be found in corresponding published articles.

218 **Power plant** We developed a method of examining, screening and applying online
219 measurement data from the continuous emission monitoring systems (CEMS, Zhang
220 et al., 2019b) to estimate the emissions at the power unit/plant level. For units without
221 CEMS data, we applied the average flue gas concentrations obtained from CEMS for
222 units with the same installed capacity. The emissions were calculated based on the
223 annual mean hourly flue gas concentration of air pollutant obtained from CEMS and
224 the theoretical annual flue gas volume of each unit/plant:

$$225 \quad E_{i,j} = C_{i,j} \times AL_j \times V_m^0 \quad (1)$$

226 where E is the emission of air pollutant; i, j and m represent the pollutant species,
227 individual plant/unit, and fuel type, respectively; C is the annual average



228 concentration in the flue gas; AL is the annual coal consumption, and V^0 is the
229 theoretical flue gas volume per unit of fuel consumption, which depends on the coal
230 type and can be calculated following the method in Zhao et al. (2010).

231 **Industrial plant** Emissions were principally calculated based on activity level data
232 (production output or energy consumption) and emission factor (emissions per unit of
233 activity level). For point sources with abundant information, we used a
234 procedure-based approach to calculate the emissions of pollutants (Zhao et al., 2017).
235 For example, we subdivided the iron and steel industry into sintering, pelletizing, iron
236 making, steel making, rolling steel, and coking. The activity data and emission factors
237 of each procedure were derived based on multiple information collected from
238 enterprise regular report, statistics, and/or on-site investigation at the facility level (see
239 Section 2.1.3). The emissions of air pollutants were calculated using Eq. (2):

$$240 \quad E_i = \sum_{j,r} AL_{j,r} \times EF_{i,j,r} \times (1 - \eta_{i,j,r}) \quad (2)$$

241 where r is the industrial procedure; AL is the activity level; EF is the unabated
242 emission factor; η is the pollutant removal efficiency of end-of-pipe control
243 equipment.

244 **Petrochemical industry** Certain procedures in petrochemical industry have been
245 identified as the main contributors to AVOCs emissions from the sector. For example,
246 equipment leaks, storage tanks, and manufacturing lines were estimated to be
247 responsible for over 90% of the total emissions (Ke et al., 2020; Liu et al., 2020; Yen
248 and Horng, 2009). Through field measurements and in-depth analysis of different
249 emission calculation methods, Zhang et al. (2021a) suggested that procedure-based
250 method should provide better estimate of NMVOCs emissions for petroleum
251 industries than the commonly approach that applied a full emission factor for the
252 whole factory. In this study, therefore, we applied the procedure-based method for
253 four key procedures (manufacturing lines, storage tanks, equipment leaks, and
254 wastewater collection and treatment system), with best available information from
255 on-site surveys and regular enterprise reports.

256 **Agriculture** Agricultural NH_3 emissions can be significantly influenced by the
257 meteorological, soil environment, and farming manners, and thus are more difficult to



258 track compared to SO₂ and NO_x that are largely from power and industrial plants. For
259 example, the relatively high temperature and top dressing fertilization conducted in
260 summer could significantly elevate the NH₃ volatilization for urea fertilizer use in
261 YRD. Our previous work (Zhao et al., 2020) quantified the effects of metrology, soil
262 property and various agricultural processes (e.g., fertilizer use and manure
263 management) on YRD NH₃ emissions for 2014. Here we expanded the research period
264 and obtained the agricultural NH₃ emission inventory for 2015-2019 in Jiangsu.

265 **Off-road transportation** We developed a novel method to estimate the emissions and
266 their spatiotemporal distribution for in-use agricultural machinery, by combining
267 satellite data, land and soil information, and in-house investigation (Zhang et al.,
268 2020). In particular, the machinery usage was determined based on the spatial
269 distribution, growing and rotation pattern of the crops. Moreover, twelve construction
270 and agricultural machines with different power capacity and emission grades (China
271 I-III) were selected and emission factors were measured under various working loads
272 (unpublished). In this work, we combined the method developed by Zhang et al.
273 (2020) and newly tested emission factors to estimate the emissions from off-road
274 machines in Jiangsu for multiple years.

275 **Biogenic source:** Located in the subtropics, Jiangsu has abundant broadleaf
276 vegetation, a main contributor to biogenic volatile organic compounds (BVOCs)
277 emissions. Our previous work (Wang et al., 2020b) evaluated the effect of land cover
278 data, emission factors and O₃ exposure on BVOCs emissions in YRD with the Model
279 of Emissions of Gases and Aerosols from Nature (MEGAN). Here we followed the
280 improved method by Wang et al. (2020b) and calculated BVOCs emissions with
281 integrated land cover information, local BVOCs emission factors, and influence of
282 actual O₃ stress in Jiangsu.

283 **Other sources** Emissions from on-road vehicles and residential sectors were
284 estimated following our previous work (Zhou et al., 2017; Zhao et al., 2021), with
285 updated activity levels and emission factors.

286 **NMVOCs speciation** We updated NMVOCs speciation by incorporating the local
287 source profiles from field measures (Zhao et al., 2017; Zhang et al., 2021a) and



288 massive literature reviews of previous studies (Mo et al., 2016; Li et al., 2014; Huang
289 et al., 2021; Wang et al., 2020a). Compared with the widely used SPECIATE 4.4
290 database (<https://www.epa.gov/air-emissions-modeling/speciate>, Hsu et al., 2018), we
291 included new source profiles from local measurements for production of sugar,
292 vegetable oil and beer, and refined the source profiles for the use of paints, inks,
293 coatings, dyes, dyestuffs and adhesives in manufacturing industry (Zhang et al.,
294 2021a), and selected production processes of chemical engineering (Zhao et al., 2017).
295 Moreover, we split the source profiles for some categories into finer ones, for example,
296 NMVOCs release in filling station into petrol and diesel release, metal surface
297 treatment into water-based and solvent-based paints, and ink printing into offset,
298 gravure and letterpress printing. Those efforts made the NMVOCs speciation more
299 representative for local emission sources (Zhang et al., 2021a).

300 **2.1.3 Data compilation, investigation and incorporation**

301 In this study, we compiled, investigated and incorporated most available information
302 on emission sources to improve the completeness, representativeness and reliability of
303 provincial emission inventory. In particular, we collected officially reported
304 Environmental Statistics Database (ESD, 2015-2019) and the Second National
305 Pollution Source Census (SNPSC, 2017) for information of stationary sources (mostly
306 power and industrial ones). Both of them contained basic information on location, raw
307 material and energy consumption, product output, and manufacturing and emission
308 control technologies. The former was routinely reported for relatively big point
309 sources every year, but some information could be outdated or inaccurate attributed to
310 insufficient on-site inspection. Through wide on-site surveys, in contrast, the latter
311 included much more plants, and provided or corrected crucial information at facility
312 level, such as removal efficiency of air pollutant control devices (APCD). However,
313 the database was developed for 2017 and could not track the changes for recent years.
314 Therefore, we further applied an internal database from the Air Pollution Source
315 Emission Inventory Compilation and Analysis System (APSEICAS,



316 <http://123.127.175.61:31000>), which was developed by Jiangsu Provincial Academy
317 of Environmental Sciences. Following the principal of SNPSC, the information of
318 APSEICAS has been collected and dynamically updated since 2018, based mainly on
319 in-depth investigation for individual enterprises conducted jointly by themselves and
320 local environmental administrators. We made cross validation and necessary revision
321 according to above-mentioned three databases, to ensure the accuracy of information
322 as much as possible.

323 As a result, we obtained sufficient numbers of point sources with satisfying
324 facility-level information for provincial-level emission inventory development
325 (57,457, 32,324 and 48,826 for 2017, 2018, and 2019, respectively). The shares of
326 coal consumption by those sources to the total ranged 90-94% for the three years. The
327 high proportions of point sources could effectively reduce the uncertainty in
328 estimation and spatial allocation of air pollutant emissions. For the remaining
329 industrial sources, the emissions were calculated with the average emission factor by
330 city and sector, and were spatially allocated according to the distribution of local
331 industrial parks and GDP.

332 Other information including area industrial sources, transportation, agricultural, and
333 residential sources were taken from economical and energy statistical yearbooks at
334 city level. Activity data that were not recorded (e.g., civil solvent usage, catering, and
335 biomass burning) were indirectly estimated from relevant statistics, including
336 population, building area, and crop yields.

337 **2.2 Analysis of emission change**

338 In this study, we summarized 13 major control measures adopted between 2015 and
339 2019, based on NAPAPCP, TYAPFAP and relative action plans promulgated by the
340 Jiangsu government (Figure S2 in the Supplement). Those included Ultra-low
341 emission retrofit of coal-fired power plants, Extensive management of coal-fired
342 boilers, Upgradation and renovation of non-electrical industry, Phasing out outdated
343 industrial capacities, Promoting clean energy use, Phasing out small polluting



344 factories, Construction of port shore power, Comprehensive treatment of mobile
345 source pollution, VOCs emission control in key sectors, Application of leak detection
346 and repair (LDAR), Oil and gas recovery, Replacement with low-VOC paints, Control
347 of non-point pollution. We applied the method by Zhang et al. (2019a) to quantify the
348 benefits of those air clean actions on emission abatement. Briefly, the emission
349 reduction resulting from implementation of a specific measure was estimated by
350 changing the parameters of emission calculation associated with the measure within
351 the concerned period, and keeping other parameters constant (same as initial year).
352 The emission reduction from each measure was then estimated for 2015-2017 and
353 2017-2019. The provincial-level emission inventory developed in Section 2.1 was
354 adopted as the baseline of the emission estimates. It was worth noting that the
355 aggregated emission reduction from all the measures did not equal to the net reduction,
356 as the factors leading to emission growth were not counted in this analysis.

357 **2.3 Air quality modeling**

358 **2.3.1 Model configurations**

359 To evaluate the provincial-level emission inventory, we used the Community
360 Multiscale Air Quality (CMAQ v5.1) model developed by US Environmental
361 Protection Agency (USEPA), to simulate the PM_{2.5} and O₃ concentrations in Jiangsu.
362 Four months (January, April, July, and October) of each year between 2015 and 2019
363 were selected as the simulation periods, with a spin-up time of 7 days for each month
364 to reduce the impact of the initial condition on the simulation. As shown in Figure S1,
365 three nested domains (D1, D2, and D3) were applied with the horizontal resolutions at
366 27, 9, and 3 km, respectively, and the most inner D3 covered Jiangsu and parts of the
367 YRD region including Shanghai, northern Zhejiang, and eastern Anhui. MEIC was
368 applied for D1, D2, and the regions out of Jiangsu in D3, and the provincial-level
369 emission inventory was applied for Jiangsu in D3. The Carbon Bond Mechanism
370 (CB05) and AERO5 mechanisms were used for the gas-phase chemistry and aerosol
371 module, respectively.



372 The meteorological field for the CMAQ model was obtained from the Weather
373 Research and Forecasting model (WRF v3.4). Meteorological initial and boundary
374 conditions were obtained from the National Centers for Environmental Prediction
375 (NCEP) datasets. Ground observations at 3-h intervals were downloaded from
376 National Climatic Data Center (NCDC). Statistical indicators including bias, index of
377 agreement (IOA), and root mean squared error (RMSE) were used to evaluate the
378 WRF performance (Yang et al., 2021a). The discrepancies between simulations and
379 ground observations were within an acceptable range (Table S2 in the Supplement).

380 In order to evaluate the model performance of CMAQ, we collected ground
381 observation data of hourly PM_{2.5} and O₃ concentrations at the 110 state-operating air
382 quality monitoring stations within Jiangsu (<https://data.epmap.org/page/index>, see the
383 station locations in Figure S1). Correlation coefficients (R), normalized mean bias
384 (NMB) and normalized mean errors (NME) between observation and simulation for
385 each month were calculated to evaluate the performance of CMAQ modeling:

$$386 \quad NMB = \frac{\sum_{p=1}^n (S_p - O_p)}{\sum_{p=1}^n O_p} \times 100\% \quad (3)$$

$$387 \quad NME = \frac{\sum_{p=1}^n |S_p - O_p|}{\sum_{p=1}^n O_p} \times 100\% \quad (4)$$

388 where S and O are the simulated and observed concentration of air pollutant,
389 respectively, and p indicates the individual year ($n=5$ in this study).

390 We further compared the modeling performance using provincial-level emission
391 inventory in D3 with that using MEIC in D2. Zheng et al. (2017) suggested a much
392 larger bias for high-resolution simulation (additional 8-73% at 4 km) than that at
393 coarser resolution (3-13% for 36 km) when MEIC was applied in predicting surface
394 concentrations of different air pollutants. To avoid expanded modeling bias, therefore,
395 we did not directly downscale MEIC into the entire D3.

396 **2.3.2 Emission and meteorological factors affecting the variation of PM_{2.5} and O₃**

397 We set up different scenarios to assess the impacts of emission and meteorological
398 changes on the interannual variations of PM_{2.5} and O₃ concentrations, and to reveal
399 their varying contributions for different periods. The baseline represented the



400 simulation for 2015, 2017, and 2019 with the emission inventory and meteorological
401 fields for corresponding year. The meteorological variation scenario (VMET) used the
402 varying meteorological fields for the three years but fixed the emission input at the
403 2017 level, and was thus able to quantify the impact of changing meteorological
404 conditions on PM_{2.5} and O₃ concentrations. For example, the difference between 2015
405 and 2017 in VMET indicated the contribution of changing meteorology to variation of
406 air pollutant concentration (same for the period 2017-2019). Similarly, the emission
407 variation scenario (VEMIS) used the varying emission inventory for the three years
408 but fixed meteorological fields at the 2017 level, and was thus able to quantify the
409 impact of changing emissions on PM_{2.5} and O₃ concentrations. For example, the
410 difference between 2015 and 2017 in VEMIS indicated the contribution of changing
411 emissions to variation of air pollutant concentration (same for the period 2017-2019).
412 The contributions between 2015 and 2017, and those between 2017 and 2019, could
413 then be compared to evaluate the effectiveness of emission control on air quality for
414 the two periods. Notably the emission change in the modeling scenario referred to that
415 for entire D3, thus the contribution of emission control to the changing air quality
416 included both from Jiangsu and nearby regions. Given the clearly larger emission
417 intensity for the former compared to the latter (An et al., 2021), the contribution of
418 local emissions was expected to be more important on the air quality than regional
419 transport.

420 **3. Results and discussions**

421 **3.1 Air pollutant emissions by sector and region**

422 **3.1.1 Anthropogenic emission changes by sector**

423 From 2015 to 2019, the total emissions of anthropogenic SO₂, NO_x, AVOCs, NH₃,
424 CO, PM₁₀, PM_{2.5}, BC, and OC in Jiangsu were estimated to decline 53%, 20%, 6%,
425 10%, 7%, 21%, 16%, 6% and 18%, down to 296, 1122, 1271, 422, 7163, 565, 411, 32,
426 and 36 Gg in 2019, respectively (Table S3 in the Supplement). On top of SO₂ and



427 NO_x, NMVOCs has been incorporated into national economic and social
428 development plans with emission reduction targets in China since 2015, because of its
429 harmful impact on human health and increasingly important role on triggering O₃
430 formation. The central government required the total national emissions of SO₂, NO_x,
431 and NMVOCs to be cut by 15%, 15%, and 10% during the 13th Five-Year Plan period
432 (2015-2020), respectively (Zhang et al., 2022). Our estimates show that the actual SO₂
433 and NO_x emission reductions were larger than planned in Jiangsu, due to the
434 implementation of stringent pollution control measures. However, AVOCs emissions
435 did not decline considerably within the research period, resulting from less
436 penetration of efficient APCD, and more fugitive leakage that were difficult to capture.
437 Relatively small reductions were also found for BC and CO, which are closely
438 associated with incomplete combustion of small-scale sources and vehicles. The lack
439 of APCD and growth of vehicle use were expected to offset the benefits of emission
440 controls for other sectors. As shown in Figure 1, the GDP and vehicle population grew
441 40% and 24%, respectively, while coal consumption declined slightly during
442 2015-2019. Along with stringent emission reduction actions, the provincial emissions
443 of SO₂, NO_x and PM_{2.5} were clearly decoupling from those economical and energy
444 factors, while CO was still strongly influenced by the change of coal consumption.

445 We present the sectoral contribution to anthropogenic emissions and their interannual
446 changes in Figure 2 and Figure 3, respectively. Industrial sector was identify as the
447 major contributor to SO₂, CO, AVOCs, PM₁₀, and PM_{2.5} emissions, accounting
448 averagely for 50%, 62%, 64%, 68%, and 61% of them during 2015-2019, respectively
449 (Figure 2a, c, d, f and g). The sector was found to drive the reductions in emissions of
450 SO₂, NO_x, CO, PM₁₀, PM_{2.5} and BC. In particular, the benefit of emission controls on
451 industrial sector after 2017 was found to clearly elevated and to surpass that of power
452 sector for SO₂, NO_x, PM₁₀ and PM_{2.5} (Figure 3a, b, f and g).

453 The power sector, accounting for more than half of provincial coal burning though,
454 was not the most important contributor to the emissions of any pollutant (Figure 2).
455 Upgrading the units with advanced APCDs, phasing-out outdated boilers, and
456 retrofitting for ultra-low emission requirement significantly reduced SO₂, NO_x, and



457 particulate emissions from the power sector (Liu et al., 2015; Zhang et al., 2021b).
458 With the completion of the ultra-low emission retrofit in 2017, the declines of
459 emissions for most species slowed down for the power sector (Figure 3). The results
460 indicated that the potential for further emission abatement from end-of-pipe controls
461 has been very limited for the sector, unless an energy transition with less coal
462 consumption is sustainably undertaken in Jiangsu.

463 The transportation sector averagely accounted for 51%, 17%, 14% and 42% of NO_x,
464 CO, AVOCs and BC emissions, respectively (Figure 2b, c, d, and h). The growth of
465 vehicle population resulted in a 38% increase in the annual NO_x emissions from
466 transportation from 2015 to 2019, faster than that of any other sector (Figure 3b).
467 Similarly, a 20% and 25% increase were found for transportation CO and BC
468 emissions (Figure 3c and h), respectively. Therefore, the rapid development of
469 transportation in economically developed Jiangsu has expanded its contribution to air
470 pollutant emissions for those species, particularly after the emissions from large
471 power and industrial plants have been effectively curbed. However, implementation of
472 China V emission standard (equal to Euro V,
473 <https://publications.jrc.ec.europa.eu/repository/handle/JRC102115>) for motor vehicles
474 since 2018 effectively slowed down the growth of transportation NO_x emissions: The
475 annual growth rate was estimated to decrease from 12% for 2015-2017 to 5% in
476 2018-2019. Meanwhile, a downward trend was also found for transportation AVOCs
477 emissions since 2018 (Figure 3d). Those results show that emission controls for
478 transportation could be crucial for limiting the key precursors of ozone production
479 (Geng et al., 2021; Zhang et al., 2019a).

480 The residential sector was the most important source of OC, contributing averagely 68%
481 to total emissions within 2015-2019 (Figure 2i), and was the second most important
482 source of PM₁₀ (18%, Figure 2f) and PM_{2.5} (24%, Figure 2g). It dominated the
483 abatement of OC emissions, attributed to the reduced bulk coal and straw burning
484 (Figure 3i). The agricultural sector dominated NH₃ emissions (91%, Figure 2e), and
485 the small decline resulted mainly from the reduced use of nitrogen fertilizer (13%)
486 from 2015 to 2019 (Figure 3e).



487 **3.1.2 City-level emissions and spatial distribution**

488 Figure 4 shows the average annual emissions of SO₂, NO_x, AVOCs, NH₃, PM_{2.5} for
489 the five years by city. Clearly larger emissions of most species were found in southern
490 Jiangsu cities (see the city definitions in Figure S1) with more developed industrial
491 economy and transportation (Figure 4a-e, see the detailed emission data by year and
492 city in Table S4 in the Supplement). The SO₂ emissions per unit area were calculated
493 at 7.7, 3.3, and 2.4 ton·km⁻² for southern, central and northern cities, respectively. The
494 analogous numbers were 23.0, 11.7, and 8.1 ton·km⁻² for NO_x, 22.5, 13.2, and 8.1
495 ton·km⁻² for AVOCs, and 7.3, 5.2, and 2.9 ton·km⁻² for PM_{2.5}, respectively. As shown
496 in Figure S3 in the Supplement, the regions along the Yangtze River were of largest
497 densities of power and industrial plants. In contrast, higher NH₃ emissions were found
498 for central and northern cities with abundant agricultural activities (Figure 4). Figure
499 S4 in the Supplement illustrates the spatial distributions of emissions for selected
500 species for 2019, at a horizontal resolution of 3km. Besides industrial sources, the
501 spatial patterns of NO_x, BC, CO and AVOCs were also influenced by the road net,
502 suggesting the role of heavy traffic on emissions. Particulate matter emissions were
503 mainly distributed in urban industrial regions, while OC was more found in broader
504 central and northern areas, attributed partly to the contribution from residential biofuel
505 use.

506 As shown in Figure 4, the emission fractions of southern cities decreased from 2015
507 to 2019 except for AVOCs and NH₃, indicating more benefits of stringent measures on
508 emission controls for relatively developed regions. Faster declines in annual SO₂,
509 NO_x and PM_{2.5} emissions for southern cities (59%, 23%, and 24% from 2015 to 2019,
510 respectively) were estimated than northern cities (53%, 18%, and 8%, respectively).
511 In contrast, AVOCs emissions were estimated to increase by 10% in southern cities
512 while decrease by 27% in northern cities.

513 Figure 5 illustrates the changes in spatial distribution of major pollutant emissions
514 from 2015 to 2019 in Jiangsu. It can be found that the areas with large emission
515 reduction for SO₂, NO_x, and PM_{2.5} were consistent with the locations of super



516 emitters of corresponding species (Figure 5a-c). Facing bigger challenges in air
517 quality improvement, more efforts have been made on the emission controls of
518 large-scale power and industrial enterprises in the economically developed southern
519 Jiangsu, leading to greater emission reduction compared to less developed northern
520 Jiangsu. Opposite pattern in spatial variation of emissions was found for AVOCs
521 (Figure 5d). There was a big development of industrial parks for chemical engineering
522 along the riverside of Yangtze River in the cities of Suzhou, Nantong, and Wuxi in
523 southern Jiangsu. The elevated solvent use and output of chemical products of those
524 large-scale enterprises resulted in the growth of AVOCs emissions. In northern
525 Jiangsu, in contrast, small-scale chemical plants have been gradually closed, and the
526 emissions were thus effectively reduced. There is a thus great need for substantial
527 improvement of emission controls for the key regions and sectors for further
528 abatement of AVOCs emissions.

529 **3.1.3 Enhanced contribution of biogenic sources to total NMVOCs**

530 Table 1 summarizes AVOCs and BVOCs emissions by month and year. Different from
531 AVOCs that decreased slowly but continuously from 2015 to 2019, a clearly growth
532 of annual BVOCs emissions was estimated between 2015 and 2017, followed by a
533 slight reduction till 2019. The peak annual BVOCs emissions reached 213 Gg in 2017.
534 The interannual variation of BVOCs was mainly associated to that of temperature and
535 short-wave radiation (Wang et al., 2020b). Influenced by meteorological conditions
536 and vegetation growing season, BVOCs emissions were most abundant in July, less in
537 April and October and almost zero in January. Within the province, there existed a
538 general increasing gradient from southeast to northwest in BVOCs emissions (Figure
539 S5 in the Supplement). The rapid development of industrial economy in southern
540 Jiangsu has led to the expansion of urban centers and less vegetation cover, which
541 limited the BVOCs emissions.
542 We calculated the ratio of BVOCs to AVOCs emissions by month and year (Table 1).
543 Dependent on the emission trends of both BVOCs and AVOCs, the annual ratio



544 gradually increased from 11 in 2015 to 16 in 2017, and stayed above 15 afterwards.
545 There is also a clear seasonal difference in the ratio, with the averages for the five
546 years estimated at 0%, 8%, 52%, and 3% for January, April, July and October,
547 respectively. Since 2016, the ratio of BVOCs to AVOCs emissions exceeded 50% in
548 July, indicating that the O₃ pollution in summer could be increasingly influenced by
549 BVOCs. Regarding the spatial pattern, larger ratios were commonly found in northern
550 Jiangsu, with a modest growth for recent years (Figure 6). Moreover, greater growth
551 of the ratio was found in part of southern Jiangsu where AVOCs emissions were
552 rapidly declining (e.g., Nanjing and Zhenjiang). The evolution indicated that biogenic
553 sources gradually became more influential in O₃ production even for some regions
554 with developed industrial economy, along with controls of anthropogenic emissions.
555 Due to the relatively high level of ambient NO₂ from anthropogenic emissions, a
556 broad areas of Jiangsu were identified with a mixed or VOC-limited regime in terms
557 of O₃ formation (Jin and Holloway, 2015), indicating the impacts of NMVOCs
558 (including BVOCs) on the ambient O₃ concentration. In the future, the BVOCs
559 emissions may further increase with the elevated temperature, improved afforestation
560 and vegetation protection, and they will probably play a more important role on
561 summer O₃ pollution once the controls of AVOCs emissions are pushed forward (Ren
562 et al., 2017; Gao et al., 2022a).

563 **3.2 Influence of different data and methods on emission estimates**

564 **3.2.1 Assessment of interannual variability**

565 Figure 7 compares the interannual trends of SO₂ and NO_x emissions estimated in this
566 study with those in available global (EDGAR) and national emission inventories
567 (MEIC), as well as those of annual averages of ambient concentrations for
568 corresponding species collected from the state-operating observation sites in Jiangsu.
569 Significantly different from other inventories, the global emission inventory EDGAR
570 could not reflect the rapid decline of SO₂ and NO_x emissions of Jiangsu for recent
571 years. It was probably due to the lack of information on the gradually enhanced



572 penetrations and removal efficiencies of APCDs use in power and industrial sectors in
573 EDGAR.

574 Both MEIC and our provincial inventory show the continuous declines in SO₂ and
575 NO_x emissions for Jiangsu from 2015 to 2019, which could be partly confirmed by
576 the ground observation. In general quite similar trends were found for the two
577 inventories, suggesting similar estimations in the interannual variation of total
578 emissions at the national and provincial scales. However, there existed some
579 discrepancies between the two. Compared to MEIC, as shown in Figure 7a, a slower
580 decline in SO₂ emissions between 2015 and 2017 was estimated by our provincial
581 inventory, but a faster one between 2017 and 2019. In other words, MEIC was more
582 optimistic in emission abatement for earlier years. The ultra-low emission retrofit on
583 power sector started from 2015 in Jiangsu, which was expected to largely reduce the
584 emissions of coal-fired plants to the level of gas-fired ones. Through investigations
585 and examinations of information on APCD operations for individual sources, we
586 cautiously speculated that the benefit of the retrofit might not be as large as expected
587 at the initial stage. This could be partly supported by the correspondence between
588 online monitoring of SO₂ emissions for individual power plants and satellite-derived
589 SO₂ columns around them when the ultra-low emission retrofit was required (Karpplus
590 et al., 2018). From 2017 to 2019, we were more optimistic on the emission reduction,
591 attributed partly to larger benefit of emission controls on non-electric industries.
592 Similar case with less discrepancy could also be found for NO_x emission (Figure 7b).

593 **3.2.2 Comparisons with previous studies**

594 To further evaluate the influence of data and methods on emission estimation, we
595 compared our provincial-level emission inventory with previous studies on emissions
596 in Jiangsu in terms of the total and sectoral emissions through examinations of activity
597 data, emission factor, removal efficiency and other parameters.

598 Table 2 compares our emission estimates, by year and species, with available
599 continental (REAS, Kurokawa et al., 2020), national (MEIC), and regional emissions



600 inventories (Li et al., 2018; Sun et al., 2018; Zhang et al., 2017b; Simayi et al., 2019;
601 An et al., 2021; Gao et al. 2022b). In particular, we stressed the differences in
602 emissions by sector among our study, MEIC and An et al. (2021) for 2017 as an
603 example (Figure 8).

604 The annual SO₂ emissions in our provincial inventory were close to those in REAS
605 (2015) and MEIC for most years, but much smaller than those reported by Sun et al.
606 (2018) and Li et al. (2018). The emissions in this work were 32% higher than the
607 MEIC for 2017, with the biggest difference (62% higher in this work) for power
608 sector (Figure 8). It resulted mainly from the discrepancies in the penetration and SO₂
609 removal efficiency of flue gas desulfurization (FGD) systems applied in the two
610 emission inventories. For example, Zhang et al. (2019a) assumed that the penetration
611 rate of FGD in the coal-fired power sector reached 99.6% in 2017, with the removal
612 efficiency estimated at 95%. According to our unit-based investigation, the removal
613 efficiencies in the power sector were typically less than 92%, owing to the aging
614 devices, low flue gas temperature and other reasons. The main differences between
615 this work and the YRD emission inventory by An et al. (2021) existed in the industrial
616 sector, attributed partly to insufficient consideration of the comprehensive emission
617 control regulations of coal-fired boilers in Jiangsu in the past few years in An et al.
618 (2021).

619 The estimates of NO_x emissions from MEIC and Sun et al. (2018) were 14-26%
620 higher than ours. The major difference between MEIC and our provincial inventory
621 existed in the power and industrial sector, and the total emissions in the former were
622 56% larger than the latter (Figure 8). For example, the emission factors for coal-fired
623 power plants in this study were derived from CEMS (0.03-2.8 g·kg⁻¹ coal),
624 significantly smaller than those from applied in MEIC and other research (2.88-8.12
625 g·kg⁻¹ coal, Zhang et al., 2021b). Similarly, the smaller emission factors for industrial
626 boilers derived based on on-site investigations were commonly smaller than previous
627 studies, leading to an estimation 45% smaller than MEIC for industrial sector in 2017.
628 Correspondingly, some modeling and satellite studies suggested that the NO_x
629 emissions in previous studies were overestimated partly due to less consideration of



630 improvement in NO_x control measures for coal burning sources (Zhao et al., 2018;
631 Sha et al., 2019).

632 As mentioned in Section 2.1.2, AVOCs emissions for certain industrial sources in this
633 study were estimated with a procedure-based approach, which took the removal
634 efficiencies of different technologies into account (Zhang et al., 2021a). Therefore, the
635 annual AVOCs emissions in the provincial inventory were commonly much smaller
636 than others. Without sufficient the local information, for example, Simaya et al. (2019)
637 applied the national average removal efficiencies of AVOCs in furniture
638 manufacturing, automotive manufacturing and textile dyeing industries at 18%, 28%,
639 and 30%, clearly lower than 21%, 42%, and 43% in our inventory, respectively. As a
640 result, the AVOCs emissions from industrial source in the former were 45% higher
641 than the latter.

642 NH₃ emissions in the provincial emission inventories were commonly smaller than
643 others. In particular, the estimate was less than half of that by An et al. (2021) for
644 2017 (Figure 8). The big difference resulted mainly from the methodologies. As
645 indicated by our previous study (Zhao et al., 2020), the method characterizing
646 agricultural processes usually provided smaller emission estimates than that using the
647 constant emission factors. The former detected the emission variation by season and
648 region, and was more supportive for air quality modeling with better agreement with
649 ground and satellite observation.

650 For PM emissions, our estimates were larger than MEIC, Gao et al. (2022b), and An
651 et al. (2021). The discrepancies resulted mainly from the inconsistent penetration rates
652 and removal efficiencies of dust collectors determined at national level and from
653 on-site surveys at provincial level. Taking cement as an example, all the plants were
654 assumed to be installed with dust collectors, and the national average removal
655 efficiency was determined at 99.3% in MEIC (Zhang et al., 2019a), clearly larger than
656 that in Jiangsu from plant-by-plant surveys (93%). Thus the PM₁₀ and PM_{2.5} emissions
657 from the industrial sector in this study were 197 and 113 Gg higher than MEIC for
658 2017 (Figure 8).



659 **3.3 Analysis of driving force of emission change from 2015 to 2019**

660 The actual reductions of annual SO₂, NO_x, AVOCs, NH₃, and PM_{2.5} emissions were
661 estimated at 331, 289, 77, 46, and 80 Gg from 2015 to 2019, respectively in our
662 provincial emission inventory. We analyzed the emission abatement and its driving
663 forces for two periods, 2015-2017 and 2017-2019, to represent the different influences
664 of individual measures on emissions for NAPAPCP and TYAPFAP. As shown in
665 Figure S6 in the Supplement, the actual emission reductions of SO₂ and NH₃ during
666 2015-2017 (211 and 34 Gg respectively) exceeded those during 2017-2019 (120 and
667 12 Gg, respectively). As the retrofit of ultra-low emission technologies for the power
668 sector and the modification of large-scale intensive management of livestock farming
669 in Jiangsu were basically completed between 2015 and 2017. The reductions of
670 annual NO_x, AVOCs, and PM_{2.5} emissions during 2017-2019 were significantly larger
671 (209, 72, and 57 Gg, respectively) than those during 2015-2017 (80, 5, and 23 Gg,
672 respectively), implying bigger benefits of TYAPFAP on emission controls of those
673 species.

674 Figure 9 summarizes the effect of individual measures on net emission reduction for
675 the two periods. The ultra-low emission retrofit of coal-fired power plants was
676 identified to be the most important driving factor for the reductions of SO₂ and NO_x
677 emissions during 2015-2017, responsible for 38% and 43% of the abatement for the
678 two species, respectively. By the end of 2017, more than 95% of the coal-fired power
679 plants in Jiangsu were equipped with FGD and selective catalytic/non-catalytic
680 reduction (SCR/SNCR), and 91% of coal-fired power generation capacity met the
681 ultra-low emission standards (35, 50 and 10 mg·m⁻³ for SO₂, NO_x and PM
682 concentration in the flue gas, respectively; Zhang et al., 2019a). Through the
683 information cross check and incorporation based on different emission source
684 databases as mentioned in Section 2.1.3, the average removal efficiencies of SO₂ and
685 NO_x in the coal-fired power plants were estimated to increase from 89% and 50% in
686 2015 to 94% and 63% in 2017, respectively.

687 The extensive management of coal-fired boilers was the second most important driver



688 for SO₂ and NO_x reduction and the most important driver for PM_{2.5}, contributing to
689 24%, 20% and 37% of the emission reductions for corresponding species, respectively.
690 The main actions included the elimination of 100 MW of coal-fired power generation
691 capacity and the enhanced penetrations of SO₂ and particulate control devices on large
692 coal-fired industrial boilers since the improved enforcement of the latest emission
693 standard (GB 13271–2014).

694 The upgradation and renovation of non-electrical industry contributed 18%, 15%, and
695 28% to the emission reductions for SO₂, NO_x, and PM_{2.5}, respectively. Till 2017,
696 more than 80% of steel-sintering machines and cement kilns were equipped with FGD
697 and SCR/SNCR systems. The average removal efficiency in the steel and cement
698 production increased from 48% and 43% in 2015 to 60% and 57% in 2017 for SO₂,
699 and from 45% and 38% in 2015 to 54% and 40% in 2017 for NO_x, respectively (as
700 shown in Figure S7 in the Supplement).

701 Phasing out outdated capacities in key industries including crude steel (8 million tons),
702 cement (9 million tons), flat glass (3 million weight-boxes), and other
703 energy-inefficient production capacity contributed 11%, 6%, and 11% to the emission
704 reductions of corresponding species, respectively. Given their relatively small
705 proportions to total emissions, the contributions of other emission reduction measures
706 were less than 10%, such as promoting clean energy, phasing out small and polluting
707 factories, and the construction of port shore power.

708 The driving forces of emission abatement have been changing since implementation
709 of TYAPFAP. The potential for further reduction of SO₂ and NO_x emissions were
710 significantly narrowed through the end-of-pipe treatment in the power sector, and the
711 ultra-emission retrofit on the sector was of very limited influence on the emissions
712 during 2017-2019. Measures on the non-electric sector brought greater benefits on
713 emission reduction. Extensive management of coal-fired boilers and upgradation and
714 renovation of non-electrical industry maintained as the most important driving factors
715 for the reduction of SO₂, NO_x, and PM_{2.5} emissions (33%, 20%, and 26% for the
716 former and 28%, 29% and 33% for the latter, respectively). After 2017, small coal



717 boilers (≤ 30 MW) were continuously shut down and remaining larger ones (≥ 60
718 MW) were all retrofitted with ultra-low emission technology. Through the ultra-low
719 emission retrofit, the average removal efficiencies of NO_x in the steel and cement
720 production increased from 54% and 40% in 2017 to 70% and 61% in 2019,
721 respectively.

722 AVOCs emission reduction resulted mainly from implementation of controls on the
723 key sectors, which accounted for 63% and 34% of the reduced emissions for
724 2015-2017 and 2017-2019, respectively. Besides, application of LDAR was the
725 second most important measure for 2015-2017, with the contribution to emission
726 reduction reaching 23%. The results also showed that AVOCs emission reductions
727 from all the concerned measures in 2017-2019 (152Gg) were higher than those in
728 2015-2017 (116 Gg). Although more abatement in total AVOCs emissions was found
729 for 2017-2019 (Figure S6), the contributions of above-mentioned two measures
730 reduced clearly in the period. Some other measures were identified to be important
731 drivers of emission reduction, including control on mobile sources (e.g.,
732 implementation of the China V emission standard for on-road vehicles) and
733 replacement with low-VOCs paints. In our recent studies, we evaluated the average
734 removal efficiency of AVOCs in industrial sector was less than 30% (Zhang et al.,
735 2021a), and organic solvents with low-VOCs content accounted for less than 30% of
736 total solvent use (Wu et al., 2022). Therefore, there would still be great potential for
737 further reduction of AVOCs emissions through improvement on the end-of-pipe
738 emission controls and use of cleaner solvents.

739 In a summary, expanding the end-of-pipe treatment (e.g., the ultra-low emission
740 retrofit) from power to non-electricity industry and phasing out the outdated industrial
741 capacities have been driving the declines of emissions for most species. Along with
742 the limited potential for current measures, more substantial improvement of energy
743 and industrial structures could be the option for further emission reduction in the
744 future.



745 **3.4 Effectiveness of emission controls on the changing air quality**

746 **3.4.1 Simulation of the O₃ and PM_{2.5} concentration**

747 The CMAQ model performance was evaluated with available ground observation.
748 The observed concentrations of PM_{2.5} (hourly) and O₃ (the maximum daily 8-h
749 average, MDA8) were compared with the simulations using the provincial emission
750 inventory and MEIC for the selected four months for 2015-2019, as summarized in
751 Table S5 and Table S6 in the Supplement. Overall, the simulation with the provincial
752 inventory shows acceptable agreement with the observations, with the annual means
753 of NMB and NME ranging -21% – 2% and 43% – 52% for PM_{2.5}, and -26% – -14%
754 and 30% – 41% for O₃. The analogous numbers for MEIC were -23% – -5% and 47%
755 – 53% for PM_{2.5}, and -26% – -6% and 33% – 46% for O₃, respectively. Most of the
756 NMB and NME were within the proposed criteria (-30% ≤ NMB ≤ 30% and NME ≤ 50%,
757 Emery et al., 2017). Better performance was achieved using the provincial inventory,
758 implying the benefit of application of refined emission data on high-resolution air
759 quality simulation.

760 Figure 10 compares the observed and simulated (with the provincial inventory)
761 interannual trends in PM_{2.5} and MDA8 O₃ concentrations from 2015 to 2019 (see the
762 simulated spatiotemporal evolution in Figures S8 and S9 in the Supplement).
763 Satisfying correlations between observed and simulated concentrations were found for
764 both PM_{2.5} and MDA8 O₃, with the squares of correlation coefficients (R²) estimated
765 at 0.81 and 0.86 within the research period, respectively. The good agreement
766 suggested the simulation with high-resolution emission inventory was able to well
767 capture the interannual changes in air quality at the provincial scale.

768 Both observation and simulation indicated a declining trend of PM_{2.5} concentrations,
769 with the annual decreasing rates estimated at -5.4 and -4.2 μg·m⁻³·yr⁻¹, respectively
770 (Figure 10a). The decline reflected the benefit of improved implementation of
771 emission control actions as well as the influence of meteorological condition change.
772 In general, higher concentrations were found in summer and lower in winter. A



773 rebound in $PM_{2.5}$ level was notably found in winter after 2017, attributed possibly to
774 the unfavorable meteorological conditions for recent years. In contrast to $PM_{2.5}$,
775 MDA8 O_3 was clearly elevated from 2015 to 2019, with the annual growth rates
776 estimated at 4.6 and 7.3 $\mu\text{g}\cdot\text{m}^{-3}\cdot\text{yr}^{-1}$, by observation and simulation (Figure 10b).
777 Higher levels were found in spring and summer and lower in autumn and winter.
778 Besides the impact of emission change, the O_3 concentrations can be greatly
779 influenced by the varying meteorological factors such as the decreased relative
780 humidity and wind speed for recent years in YRD region (Gao et al., 2021; Dang et al.,
781 2021). In addition, the recent declining $PM_{2.5}$ concentration in eastern China reduced
782 the heterogeneous absorption of hydroperoxyl (HO_2) radicals by aerosols and thereby
783 enhanced O_3 concentration (Li et al., 2019). The complicated impacts of various
784 factors on air quality triggered the separation of emission and meteorological
785 contributions to the changing $PM_{2.5}$ and O_3 levels in Section 3.4.2.

786 The common underestimation of O_3 should be stressed, partly resulting from the bias
787 in the estimation of precursor emissions. In this study, the enhanced penetrations
788 and/or removal efficiencies of NO_x control devices might not be fully considered in
789 the emission inventory development, in particular for the non-electric industry,
790 leading to possible overestimation of NO_x emissions. Moreover, underestimation of
791 AVOCs emissions could exist, due to incomplete counting of emission sources,
792 particularly for the uncontrolled fugitive leakage. As most of Jiangsu was identified as
793 a VOC-limited region for O_3 formation (Wang et al., 2020b; Yang et al., 2021b), the
794 overestimation of NO_x and underestimation of AVOCs could resulted in
795 underestimation in O_3 concentration with air quality modeling. Furthermore, a larger
796 underestimation in O_3 was revealed before 2017 (Figure 8b), attributed partly to less
797 data support on the emission sources and thereby less reliability in the emission
798 inventory, compared with more recent years.

799 **3.4.2 Anthropogenic and meteorological contribution to O_3 and $PM_{2.5}$ variation**

800 Figure 11 explores the effects of the changing anthropogenic emissions (VEIMS) and



801 meteorology (VMET) on PM_{2.5} and MDA8 O₃ levels in 2015-2017 and 2017-2019. In
802 the baseline that contained the interannual changes of both factors, the
803 provincial-level PM_{2.5} concentration was simulated to decrease by 4.1 μg·m⁻³ in
804 2015-2017 and 1.7 μg·m⁻³ in 2017-2019, and MDA8 O₃ increase by 17.0 μg·m⁻³ in
805 2015-2017 and 3.2 μg·m⁻³ in 2017-2019. Therefore, smaller variations were found for
806 more recent years for both species. Due to nonlinearity effect of the chemistry
807 transport modeling, the air quality changes in baseline did not equal to the aggregated
808 contributions in VMET and VEMIS.

809 As shown in Figure 11a, similar patterns of driving factor contributions to PM_{2.5} were
810 found between 2015-2017 and 2017-2019. While meteorological conditions
811 consistently promoted the formation of PM_{2.5}, the continuous abatement of
812 anthropogenic emissions completely offset the adverse meteorological effects and
813 contributed significantly to the declines in PM_{2.5} concentrations. Although less
814 reduction in PM_{2.5} concentration was found for 2017-2019 due mainly to the worsened
815 meteorology, emission abatement were estimated to play a greater role on reducing
816 PM_{2.5} concentration (5.5 μg·m⁻³ in VEMIS) compared to 2015-2017 (4.3 μg·m⁻³),
817 implying the bigger effectiveness of recent emission control actions on PM_{2.5}
818 pollution alleviation.

819 The O₃ case is different (Figure 11b). Both the changing emissions and meteorology
820 favored MDA8 O₃ increase for 2015-2017, consistent with previous studies (Wang et
821 al., 2019; Dang et al., 2021). The contribution of meteorology was estimated at 11.9
822 μg·m⁻³ (VMET), larger than that of emissions at 4.9 μg·m⁻³ (VEMIS). As shown in
823 Figure S6, the abatement of annual NO_x emissions in Jiangsu was estimated at 104
824 Gg, while very limited reduction was achieved in AVOCs emissions. Declining NO_x
825 emissions thus elevated O₃ formation under the VOC-limited conditions particularly
826 in urban areas in Jiangsu.

827 During 2017-2019, the meteorological condition played a more important role on the
828 O₃ growth (14.3 μg·m⁻³), attributed mainly to the decreased relative humidity and
829 wind speed for recent years (Table S2). In contrast, the changing emissions were
830 estimated to restrain the O₃ growth by 3.1 μg·m⁻³, implying the effectiveness of



831 continuous emission controls on O₃ pollution alleviation. As shown in Figure S6, a
832 much larger reduction in AVOCs emissions were achieved in Jiangsu during
833 2017-2019 compared to 2015-2017, and the greater NO_x emission reduction might
834 have led to the shift from VOC-limited to the transitional regime across the province
835 (Wang et al., 2021b). The emission controls thus helped limiting the total O₃
836 production. Although the reduction in precursor emissions was not able to fully offset
837 the effect of adverse meteorology condition, its encouraging effectiveness
838 demonstrated the validity of current emission control measures, and actual O₃ decline
839 can be expected with more stringent control actions to overcome the influence of
840 meteorological variation.

841 **4. Conclusion remarks**

842 In this study, we developed a high-resolution emission inventory of nine air pollutants
843 for Jiangsu 2015-2019, by integrating the improvements in methodology for different
844 sectors and incorporating the best available facility-level information and real-world
845 emission measurements. We evaluated this provincial-level emission inventory
846 through comparison with other studies at different spatial scales and air quality
847 modeling. We further linked the emission changes to various emission control
848 measures, and evaluated the effectiveness of pollution control efforts on the emission
849 reduction and air quality improvement.

850 Our study indicated that the emission controls indeed played an important role on
851 prevention and alleviation of air pollution. Through a series of remarkable actions in
852 NAPAPCP and TYAPFAP, the annual emissions in Jiangsu declined to varying
853 degrees for different species from 2015 to 2019, with the largest relative reduction at
854 53% for SO₂ and smallest at 6% for AVOCs. Regarding different periods, larger
855 abatement of SO₂ emissions was found between 2015 and 2017 but more substantial
856 reductions of NO_x, AVOCs and primary PM_{2.5} between 2017 and 2019. Our estimates
857 in SO₂, AVOCs and NH₃ emissions were mostly smaller than or close to other studies,
858 while those for NO_x and primary PM_{2.5} were less conclusive. The main reasons for



859 the discrepancies between studies included the modified methodologies used in this
860 work (e.g., the procedure-based approach for AVOCs and the agricultural process
861 characterization for NH₃) and the varied depths of details on emission source
862 investigation (e.g., the penetrations and removal efficiencies of APCD). Air quality
863 modeling confirmed the benefit of refined emission data on predicting the ambient
864 levels of PM_{2.5} and O₃, as well as capturing their interannual variations.
865 For 2015-2017 within NAPAPCP, the ultra-low emission retrofit on power sector was
866 most effective on SO₂ and NO_x emission reduction, but the expansion of emission
867 controls to non-electricity sectors, including coal-fired boilers and key industries
868 would be more important for 2017-2019. AVOCs control was still in its initial stage,
869 and the measures on key industrial sectors and transportation were demonstrated to be
870 effective. Along with the gradually reduced potential for emission reduction through
871 end-of-pipe treatment, adjustment of energy and industrial structures should be the
872 future path for Jiangsu as well as other regions with developed industrial economy.
873 Air quality modeling suggested worsened meteorological conditions from 2015 to
874 2019 in terms of PM_{2.5} and O₃ pollution alleviation. The continuous actions on
875 emission reduction, however, have been taking effect on reducing PM_{2.5} concentration
876 and restraining the growth of MDA8 O₃ level.
877 The analysis justified the big efforts and investments by the local government for air
878 pollution controls, and demonstrated how the investigations of detailed underlying
879 data could help improve the precision, integrity and continuity of emission inventories.
880 Such demonstration was more applicable at regional scale instead of national scale,
881 due to the huge cost and data gap for the latter. Furthermore, the work showed how
882 the refined emission data could efficiently support the high-resolution air quality
883 modeling, and highlighted the varying and complex responses of air quality to
884 different emission control efforts. Therefore, the study could shed light for other
885 highly polluted regions in China and worldwide, with diverse stages of economic
886 development and air pollution controls.
887 Limitations remain in the current study. Attributed to insufficient data support, there
888 was little improvement on emission estimation for some sources compared to previous



889 studies, e.g., on-road transportation and residential sector. Those sources may play an
890 increasingly important role on emissions and air quality along with stringent controls
891 on power and industrial sectors, and thus need to be better stressed in the future.
892 Given the limited access on emission source information, the emission data for nearby
893 regions around Jiangsu were not refined in this work. Such limitation might lead to
894 some bias in analyzing the effectiveness of emission controls on air quality, as
895 regional transport could account for a considerable fraction of PM_{2.5} and O₃
896 concentrations. Should better regional emission data get available, more analysis
897 needs to be conducted to separate the effectiveness of local emission controls and
898 efforts from nearby regions. Due to huge computational tasks through air quality
899 modeling, moreover, the individual emission control measures were not directly
900 linked to the ambient concentration, and their effectiveness on air quality
901 improvement cannot be obtained in details. Advanced numerical tools, e.g., the
902 adjoint modeling, are recommended for further in-depth analysis.

903 **Data availability**

904 The gridded emission data for Jiangsu Province 2015-2019 can be downloaded at
905 <http://www.airqualitynju.com/En/Data/List/Datadownload>

906 **Author contributions**

907 CGu developed the methodology, conducted the research and wrote the draft. YZhao
908 and LZhang developed the strategy and designed the research, and YZhao revised the
909 manuscript. ZXu provided the support of air quality modeling. YWang, ZWang and
910 HWang provided the support of emission data processing. SXia, LLi, and QZhao
911 provided the support of emission data.

912 **Competing interests**

913 The authors declare that they have no conflict of interest.



914 **Acknowledgments**

915 This work received support from the Natural Science Foundation of China
916 (42177080 and 41922052), the Jiangsu Provincial Fund on PM_{2.5} and O₃ Pollution
917 Mitigation (No. 2019023), and Key Research and Development Programme of
918 Jiangsu Province (BE2022838).

919 **References**

- 920 An, J., Huang, Y., Huang, C., Wang, X., Yan, R., Wang, Q., Wang, H., Jing, S., Zhang,
921 Y., Liu, Y., Chen, Y., Xu, C., Qiao, L., Zhou, M., Zhu, S., Hu, Q., Lu, J., and
922 Chen, C.: Emission inventory of air pollutants and chemical speciation for
923 specific anthropogenic sources based on local measurements in the Yangtze
924 River Delta region, China, *Atmos. Chem. Phys.*, 21, 2003–2025,
925 <https://doi.org/10.5194/acp-21-2003-2021>, 2021.
- 926 Crippa, M., Solazzo, E., Huang G., Guizzardi D., Koffi E., Muntean M., Schieberle C.,
927 Friedrich R.: High resolution temporal profiles in the Emissions Database for
928 Global Atmospheric Research, *Sci. Data*, 7, 121,
929 <https://doi.org/10.1038/s41597-020-0462-2>, 2020.
- 930 Dang, R., Liao, H., and Fu, Y.: Quantifying the anthropogenic and meteorological
931 influences on summertime surface ozone in China over 2012–2017, *Sci. Total*
932 *Environ.*, 754, 142394, <https://doi.org/10.1016/j.scitotenv.2020.142394>, 2021.
- 933 Emery, C., Liu, Z., Russell, A. G., Odman, M. T., Yarwood, G., and Kumar, N.:
934 Recommendations on statistics and benchmarks to assess photochemical model
935 performance, *J. Air Waste Manag. Assoc.*, 67, 582–598,
936 [10.1080/10962247.2016.1265027](https://doi.org/10.1080/10962247.2016.1265027), 2017.
- 937 Gao, D., Xie, M., Liu, J., Wang, T., Ma, C., Bai, H., Chen, X., Li, M., Zhuang, B., and
938 Li, S.: Ozone variability induced by synoptic weather patterns in warm seasons
939 of 2014–2018 over the Yangtze River Delta region, China, *Atmos. Chem. Phys.*,
940 21, 5847–5864, <https://doi.org/10.5194/acp-21-5847-2021>, 2021.



- 941 Gao, Y., Ma, M., Yan, F., Su, H., Wang, S., Liao, H., Zhao, B., Wang, X., Sun, Y.,
942 Hopkins, J. R., Chen, Q., Fu, P., Lewis, A. C., Qiu, Q., Yao, X., and Gao, H.:
943 Impacts of biogenic emissions from urban landscapes on summer ozone and
944 secondary organic aerosol formation in megacities, *Sci. Total Environ.*, 814,
945 152654, <https://doi.org/10.1016/j.scitotenv.2021.152654>, 2022a.
- 946 Gao, Y., Zhang, L., Huang, A., Kou, W., Bo, X., Cai, B., and Qu, J.: Unveiling the
947 spatial and sectoral characteristics of a high-resolution emission inventory of
948 CO₂ and air pollutants in China, *Sci. Total Environ.*, 847, 157623,
949 <https://doi.org/10.1016/j.scitotenv.2022.157623>, 2022b.
- 950 Geng, G., Zheng, Y., Zhang, Q., Xue, T., Zhao, H., Tong, D., Zheng, B., Li, M., Liu, F.,
951 Hong, C., He, K., and Davis, S. J.: Drivers of PM_{2.5} air pollution deaths in China
952 2002–2017, *Nat. Geosci.*, 14, 645–650, [10.1038/s41561-021-00792-3](https://doi.org/10.1038/s41561-021-00792-3), 2021.
- 953 He K., Zhang Q., Wang S.: Technical manual for the preparation of urban air pollution
954 Source emission inventory, China Statistics Press, Beijing, 2018 (in Chinese).
- 955 Hsu, C., Chiang, H., Shie, R., Ku, C., Lin, T., Chen, M., Chen, N., and Chen, Y.:
956 Ambient VOCs in residential areas near a large-scale petrochemical complex:
957 Spatiotemporal variation, source apportionment and health risk, *Environ. Pollut.*,
958 240, 95–104, <https://doi.org/10.1016/j.envpol.2018.04.076>, 2018.
- 959 Huang, Y., Shen, H., Chen, H., Wang, R., Zhang, Y., Su, S., Chen, Y., Lin, N., Zhuo,
960 S., Zhong, Q., Wang, X., Liu, J., Li, B., Liu, W., and Tao, S.: Quantification of
961 Global Primary Emissions of PM_{2.5}, PM₁₀, and TSP from Combustion and
962 Industrial Process Sources, *Environ. Sci. Technol.*, 48, 13834–13843,
963 [10.1021/es503696k](https://doi.org/10.1021/es503696k), 2014.
- 964 Huang, Z., Zhong, Z., Sha, Q., Xu, Y., Zhang, Z., Wu, L., Wang, Y., Zhang, L., Cui, X.,
965 Tang, M., Shi, B., Zheng, C., Li, Z., Hu, M., Bi, L., Zheng, J., and Yan, M.: An
966 updated model-ready emission inventory for Guangdong Province by
967 incorporating big data and mapping onto multiple chemical mechanisms, *Sci.*
968 *Total Environ.*, 769, 144535, <https://doi.org/10.1016/j.scitotenv.2020.144535>,
969 2021.
- 970 Hoesly, R. M., Smith, S. J., Feng, L., Klimont, Z., Janssens-Maenhout, G., Pitkanen,



- 971 T., Seibert, J. J., Vu, L., Andres, R.J., Bolt, R. M., Bond, T. C., Dawidowski, L.,
972 Kholod, N., Kurokawa, J.-I., Li, M., Liu, L., Lu, Z., Moura, M. C. P., O'Rourke,
973 P. R., and Zhang, Q.: Historical (1750–2014) anthropogenic emissions of reactive
974 gases and aerosols from the Community Emissions Data System (CEDS), *Geosci.*
975 *Model Dev.*, 11, 369–408, <https://doi.org/10.5194/gmd-11-369-2018>, 2018.
- 976 Jin, X. and Holloway, T.: Spatial and temporal variability of ozone sensitivity over
977 China observed from the Ozone Monitoring Instrument, *J. Geophys. Res.*, 120,
978 7229–7246, 10.1002/2015JD023250, 2015.
- 979 Karplus, V. J., Zhang, S., and Almond, D.: Quantifying coal power plant responses to
980 tighter SO₂ emissions standards in China, *Proc. Natl. Acad. Sci.*, 115, 7004–7009,
981 doi:10.1073/pnas.1800605115, 2018.
- 982 Ke, J., Li, S., and Zhao, D.: The application of leak detection and repair program in
983 VOCs control in China's petroleum refineries, *J. Air Waste Manag. Assoc.*, 70,
984 862–875, 10.1080/10962247.2020.1772407, 2020.
- 985 Klimont, Z., Smith, S. J., and Cofala, J.: The last decade of global anthropogenic sulfur
986 dioxide: 2000–2011 emissions, *Environ. Res. Lett.*, 8, 014003,
987 <https://doi.org/10.1088/1748-9326/8/1/014003>, 2013.
- 988 Kurokawa, J. and Ohara, T.: Long-term historical trends in air pollutant emissions in
989 Asia: Regional Emission inventory in ASia (REAS) version 3, *Atmos. Chem.*
990 *Phys.*, 20, 12761–12793, <https://doi.org/10.5194/acp-20-12761-2020>, 2020.
- 991 Li, K., Jacob, D. J., Liao, H., Shen, L., Zhang, Q., and Bates, K. H.: Anthropogenic
992 drivers of 2013–2017 trends in summer surface ozone in China, *Proc. Natl. Acad.*
993 *Sci.*, 116, 422–427, doi:10.1073/pnas.1812168116, 2019.
- 994 Li, L., An, J. Y., Zhou, M., Qiao, L. P., Zhu, S. H., Yan, R. S., Ooi, C. G., Wang, H. L.,
995 Huang, C., Huang, L., Tao, S. K., Yu, J. Z., Chan, A., Wang, Y. J., Feng, J. L.,
996 and Chen, C. H.: An integrated source apportionment methodology and its
997 application over the Yangtze River Delta region, China, *Environ. Sci. Technol.*,
998 52, 14216–14227, 10.1021/acs.est.8b01211, 2018.
- 999 Li, M., Zhang, Q., Streets, D. G., He, K. B., Cheng, Y. F., Emmons, L. K., Huo, H.,
1000 Kang, S. C., Lu, Z., Shao, M., Su, H., Yu, X., and Zhang, Y.: Mapping Asian



- 1001 anthropogenic emissions of non-methane volatile organic compounds to multiple
1002 chemical mechanisms, *Atmos. Chem. Phys.*, 14, 5617–5638,
1003 <https://doi.org/10.5194/acp-14-5617-2014>, 2014.
- 1004 Liu, F., Zhang, Q., Tong, D., Zheng, B., Li, M., Huo, H., and He, K. B.:
1005 High-resolution inventory of technologies, activities, and emissions of coal-fired
1006 power plants in China from 1990 to 2010, *Atmos. Chem. Phys.*, 15, 13299–
1007 13317, <https://doi.org/10.5194/acp-15-13299-2015>, 2015.
- 1008 Liu, Y., Han, F., Liu, W., Cui, X., Luan, X., and Cui, Z.: Process-based volatile
1009 organic compound emission inventory establishment method for the petroleum
1010 refining industry, *J. Clean. Prod.*, 263, 10.1016/j.jclepro.2020.121609, 2020.
- 1011 Liu, M., Shang, F., Lu, X., Huang, X., Song, Y., Liu, B., Zhang, Q., Liu, X., Cao, J.,
1012 Xu, T., Wang, T., Xu, Z., Xu, W., Liao, W., Kang, L., Cai, X., Zhang, H., Dai, Y.,
1013 and Zhu, T.: Unexpected response of nitrogen deposition to nitrogen oxide
1014 controls and implications for land carbon sink, *Nat. Commun.*, 13, 3126,
1015 10.1038/s41467-022-30854-y, 2022.
- 1016 Miyazaki, K., Eskes, H., Sudo, K., Folkert Boersma, K., Bowman, K., and Kanaya, Y.:
1017 Decadal changes in global surface NO_x emissions from multi-constituent
1018 satellite data assimilation, *Atmos. Chem. Phys.*, 17, 807–837,
1019 [10.5194/acp-17-807-2017](https://doi.org/10.5194/acp-17-807-2017), 2017.
- 1020 Mo, Z., Shao, M., and Lu, S.: Compilation of a source profile database for
1021 hydrocarbon and OVOC emissions in China, *Atmos. Environ.*, 143, 209–217,
1022 <https://doi.org/10.1016/j.atmosenv.2016.08.025>, 2016.
- 1023 Mo, Z., Lu, S., and Shao, M.: Volatile organic compound (VOC) emissions and health
1024 risk assessment in paint and coatings industry in the Yangtze River Delta, China,
1025 *Environ. Pollut.*, 269, 115740, <https://doi.org/10.1016/j.envpol.2020.115740>,
1026 2021.
- 1027 National Bureau of Statistics of China: Statistical Yearbook of China, China Statistics
1028 Press, Beijing, 2016–2021 (in Chinese).
- 1029 Ren, Y., Qu, Z., Du, Y., Xu, R., Ma, D., Yang, G., Shi, Y., Fan, X., Tani, A., Guo, P.,
1030 Ge, Y., and Chang, J.: Air quality and health effects of biogenic volatile organic



- 1031 compounds emissions from urban green spaces and the mitigation strategies,
1032 Environ. Pollut., 230, 849-861, <https://doi.org/10.1016/j.envpol.2017.06.049>,
1033 2017.
- 1034 Sha, T., Ma, X. Y., Jia, H. L., van der A, R. J., Ding, J. Y., Zhang, Y. L., and Chang, Y.
1035 H.: Exploring the influence of two inventories on simulated air pollutants during
1036 winter over the Yangtze River Delta, Atmos. Environ., 206, 170–182,
1037 <https://doi.org/10.1016/j.atmosenv.2019.03.006>, 2019.
- 1038 Shen, Y., Wu, Y., Chen, G., Van Grinsven, H. J. M., Wang, X., Gu, B., and Lou, X.:
1039 Non-linear increase of respiratory diseases and their costs under severe air
1040 pollution, Environ. Pollut., 224, 631-637, [10.1016/j.envpol.2017.02.047](https://doi.org/10.1016/j.envpol.2017.02.047), 2017.
- 1041 Simayi, M., Hao, Y. F., Li, J., Wu, R. R., Shi, Y. Q., Xi, Z. Y., Zhou, Y., and Xie, S. D.:
1042 Establishment of county-level emission inventory for industrial NMVOCs in
1043 China and spatial-temporal characteristics for 2010–2016, Atmos. Environ., 211,
1044 194–203, <https://doi.org/10.1016/j.atmosenv.2019.04.064>, 2019.
- 1045 State Council of the People's Republic of China. The air pollution prevention and
1046 control national action plan.
1047 http://www.gov.cn/zwggk/2013-09/12/content_2486773.htm.
- 1048 State Council of the People's Republic of China. Three-year Action Plan for
1049 Protecting Blue Sky. Central People's Government of the People's Republic of
1050 China (2018).
1051 http://www.gov.cn/zhengce/content/2018-07/03/content_5303158.htm.
- 1052 Sun, X. W., Cheng, S. Y., Lang, J. L., Ren, Z. H., and Sun, C.: Development of
1053 emissions inventory and identification of sources for priority control in the
1054 middle reaches of Yangtze River Urban Agglomerations, Sci. Total Environ., 625,
1055 155–167, [10.1016/j.scitotenv.2017.12.103](https://doi.org/10.1016/j.scitotenv.2017.12.103), 2018.
- 1056 Wang, J. D., Zhao, B., Wang, S. X., Yang, F. M., Xing, J., Morawska, L., Ding, A. J.,
1057 Kulmala, M., Kerminen, V., Kujansuu, J., Wang, Z. F., Ding, D., Zhang, X. Y.,
1058 Wang, H. B., Tian, M., Petäjä, T., Jiang, J. K., and Hao, J. M.: Particulate matter
1059 pollution over China and the effects of control policies, Sci. Total Environ., 584–
1060 585, 426–447, <https://doi.org/10.1016/j.scitotenv.2017.01.027>, 2017.



- 1061 Wang, N., Xu, J., Pei, C., Tang, R., Zhou, D., Chen, Y., Li, M., Deng, X., Deng, T.,
1062 Huang, X., and Ding, A.: Air quality during COVID-19 lockdown in the Yangtze
1063 River Delta and the Pearl River Delta: Two different responsive mechanisms to
1064 emission reductions in China, *Environ. Sci. Technol.*, 55, 5721-5730,
1065 10.1021/acs.est.0c08383, 2021a.
- 1066 Wang, P., Guo, H., Hu, J., Kota, S. H., Ying, Q., and Zhang, H.: Responses of PM_{2.5}
1067 and O₃ concentrations to changes of meteorology and emissions in China, *Sci.*
1068 *Total Environ.*, 662, 297-306, 10.1016/j.scitotenv.2019.01.227, 2019.
- 1069 Wang, R., Yuan, Z., Zheng, J., Li, C., Huang, Z., Li, W., Xie, Y., Wang, Y., Yu, K., and
1070 Duan, L.: Characterization of VOC emissions from construction machinery and
1071 river ships in the Pearl River Delta of China, *J. Environ. Sci., (China)*, 96,
1072 138-150, 10.1016/j.jes.2020.03.013, 2020a.
- 1073 Wang, W., van der A, R., Ding, J., van Weele, M., and Cheng, T.: Spatial and temporal
1074 changes of the ozone sensitivity in China based on satellite and ground-based
1075 observations, *Atmos. Chem. Phys.*, 21, 7253–7269,
1076 <https://doi.org/10.5194/acp-21-7253-2021>, 2021b.
- 1077 Wang, Y., Zhao, Y., Zhang, L., Zhang, J., and Liu, Y.: Modified regional biogenic
1078 VOC emissions with actual ozone stress and integrated land cover information: A
1079 case study in Yangtze River Delta, China, *Sci. Total Environ.*, 727, 138703,
1080 <https://doi.org/10.1016/j.scitotenv.2020.138703>, 2020b.
- 1081 Wiedinmyer, C., Yokelson, R. J., and Gullett, B. K.: Global Emissions of Trace Gases,
1082 Particulate Matter, and Hazardous Air Pollutants from Open Burning of
1083 Domestic Waste, *Environ. Sci. Technol.*, 48, 9523-9530, 10.1021/es502250z,
1084 2014.
- 1085 Wu, R., Zhao, Y., Xia, S., Hu, W., Xie, F., Zhang, Y., Sun, J., Yu, H., An, J., and Wang,
1086 Y.: Reconciling the bottom-up methodology and ground measurement constraints
1087 to improve the city-scale NMVOCs emission inventory: A case study of Nanjing,
1088 China, *Sci. Total Environ.*, 812, 152447, 10.1016/j.scitotenv.2021.152447, 2022.
- 1089 Yang, J., Zhao, Y., Cao, J., and Nielsen, C. P.: Co-benefits of carbon and pollution
1090 control policies on air quality and health till 2030 in China, *Environ. Int.*, 152,



- 1091 106482, <https://doi.org/10.1016/j.envint.2021.106482>, 2021a.
- 1092 Yang, Y., Zhao, Y., Zhang, L., Zhang, J., Huang, X., Zhao, X., Zhang, Y., Xi, M., and
1093 Lu, Y.: Improvement of the satellite-derived NO_x emissions on air quality
1094 modeling and its effect on ozone and secondary inorganic aerosol formation in
1095 the Yangtze River Delta, China, *Atmos. Chem. Phys.*, 21, 1191–1209,
1096 <https://doi.org/10.5194/acp-21-1191-2021>, 2021b.
- 1097 Yen, C. and Horng, J.: Volatile organic compounds (VOCs) emission characteristics
1098 and control strategies for a petrochemical industrial area in middle Taiwan, *J.*
1099 *Environ. Health, Part A*, 44, 1424–1429, [10.1080/10934520903217393](https://doi.org/10.1080/10934520903217393), 2009.
- 1100 Zhang, B., Wang, S., Wang, D., Wang, Q., Yang, X., and Tong, R.: Air quality changes
1101 in China 2013–2020: Effectiveness of clean coal technology policies, *J. Clean.*
1102 *Prod.*, 366, 132961, <https://doi.org/10.1016/j.jclepro.2022.132961>, 2022.
- 1103 Zhang, J., Liu, L., Zhao, Y., Li, H., Lian, Y., Zhang, Z., Huang, C., and Du, X.:
1104 Development of a high-resolution emission inventory of agricultural machinery
1105 with a novel methodology: A case study for Yangtze River Delta region, *Environ.*
1106 *Pollut.*, 266, 115075, <https://doi.org/10.1016/j.envpol.2020.115075>, 2020.
- 1107 Zhang, L., Zhu, X., Wang, Z., Zhang, J., Liu, X., and Zhao, Y.: Improved speciation
1108 profiles and estimation methodology for VOCs emissions: A case study in two
1109 chemical plants in eastern China, *Environ. Pollut.*, 291, 118192,
1110 <https://doi.org/10.1016/j.envpol.2021.118192>, 2021a.
- 1111 Zhang, S. J., Wu, Y., Zhao, B., Wu, X. M., Shu, J. W., and Hao, J. M.: City-specific
1112 vehicle emission control strategies to achieve stringent emission reduction targets
1113 in China's Yangtze River Delta region, *J. Environ. Sci.*, 51, 75–87,
1114 <https://doi.org/10.1016/j.jes.2016.06.038>, 2017a.
- 1115 Zhang, Q., Zheng, Y., Tong, D., Shao, M., Wang, S., Zhang, Y., Xu, X., Wang, J., He,
1116 H., Liu, W., Ding, Y., Lei, Y., Li, J., Wang, Z., Zhang, X., Wang, Y., Cheng, J.,
1117 Liu, Y., Shi, Q., Yan, L., Geng, G., Hong, C., Li, M., Liu, F., Zheng, B., Cao, J.,
1118 Ding, A., Gao, J., Fu, Q., Huo, J., Liu, B., Liu, Z., Yang, F., He, K., and Hao, J.:
1119 Drivers of improved PM_{2.5} air quality in China from 2013 to 2017, *Proc. Natl.*
1120 *Acad. Sci.*, 116, 24463–24469, [doi:10.1073/pnas.1907956116](https://doi.org/10.1073/pnas.1907956116), 2019a.



- 1121 Zhang, X. M., Wu, Y. Y., Liu, X. J., Reis, S., Jin, J. X., Dragosits, U., Van Damme, M.,
1122 Clarisse, L., Whitburn, S., Coheur, P., and Gu, B. J.: Ammonia emissions may be
1123 substantially underestimated in China, *Environ. Sci. Technol.*, 51, 12089–12096,
1124 10.1021/acs.est.7b02171, 2017b.
- 1125 Zhang, Y., Bo, X., Zhao, Y., and Nielsen, C. P.: Benefits of current and future policies
1126 on emissions of China's coal-fired power sector indicated by continuous emission
1127 monitoring, *Environ. Pollut.*, 251, 415–424,
1128 <https://doi.org/10.1016/j.envpol.2019.05.021>, 2019b.
- 1129 Zhang, Y., Zhao, Y., Gao, M., Bo, X., and Nielsen, C. P.: Air quality and health
1130 benefits from ultra-low emission control policy indicated by continuous emission
1131 monitoring: a case study in the Yangtze River Delta region, China, *Atmos. Chem.*
1132 *Phys.*, 21, 6411–6430, <https://doi.org/10.5194/acp-21-6411-2021>, 2021b.
- 1133 Zhao, Y., Wang, S., Nielsen, C. P., Li, X., and Hao, J.: Establishment of a database of
1134 emission factors for atmospheric pollutants from Chinese coal-fired power plants,
1135 *Atmos. Environ.*, 44, 1515–1523, <https://doi.org/10.1016/j.atmosenv.2010.01.017>,
1136 2010.
- 1137 Zhao, Y., Zhang, J., and Nielsen, C. P.: The effects of recent control policies on trends
1138 in emissions of anthropogenic atmospheric pollutants and CO₂ in China, *Atmos.*
1139 *Chem. Phys.*, 13, 487–508, 10.5194/acp-13-487-2013, 2013.
- 1140 Zhao, Y., Qiu, L. P., Xu, R. Y., Xie, F. J., Zhang, Q., Yu, Y. Y., Nielsen, C. P., Qin, H.
1141 X., Wang, H. K., Wu, X. C., Li, W. Q., and Zhang, J.: Advantages of a city-scale
1142 emission inventory for urban air quality research and policy: the case of Nanjing,
1143 a typical industrial city in the Yangtze River Delta, China, *Atmos. Chem. Phys.*,
1144 15, 12623–12644, <https://doi.org/10.5194/acp-15-12623-2015>, 2015.
- 1145 Zhao, Y., Mao, P., Zhou, Y., Yang, Y., Zhang, J., Wang, S., Dong, Y., Xie, F., Yu, Y.,
1146 and Li, W.: Improved provincial emission inventory and speciation profiles of
1147 anthropogenic non-methane volatile organic compounds: a case study for Jiangsu,
1148 China, *Atmos. Chem. Phys.*, 17, 7733–7756,
1149 <https://doi.org/10.5194/acp-17-7733-2017>, 2017.
- 1150 Zhao, Y., Xia, Y., and Zhou, Y.: Assessment of a high-resolution NO_x emission



- 1151 inventory using satellite observations: A case study of southern Jiangsu, China,
1152 Atmos. Environ., 190, 135-145, <https://doi.org/10.1016/j.atmosenv.2018.07.029>,
1153 2018.
- 1154 Zhao, Y., Yuan, M., Huang, X., Chen, F., and Zhang, J.: Quantification and evaluation
1155 of atmospheric ammonia emissions with different methods: a case study for the
1156 Yangtze River Delta region, China, Atmos. Chem. Phys., 20, 4275–4294,
1157 <https://doi.org/10.5194/acp-20-4275-2020>, 2020.
- 1158 Zhao, Y., Huang, Y., Xie, F., Huang, X., and Yang, Y.: The effect of recent controls on
1159 emissions and aerosol pollution at city scale: A case study for Nanjing, China,
1160 Atmos. Environ., 246, 118080, <https://doi.org/10.1016/j.atmosenv.2020.118080>,
1161 2021.
- 1162 Zheng, B., Zhang, Q., Tong, D., Chen, C., Hong, C., Li, M., Geng, G., Lei, Y., Huo,
1163 H., and He, K.: Resolution dependence of uncertainties in gridded emission
1164 inventories: a case study in Hebei, China, Atmos. Chem. Phys., 17, 921–933,
1165 <https://doi.org/10.5194/acp-17-921-2017>, 2017.
- 1166 Zheng, B., Tong, D., Li, M., Liu, F., Hong, C., Geng, G., Li, H., Li, X., Peng, L., Qi, J.,
1167 Yan, L., Zhang, Y., Zhao, H., Zheng, Y., He, K., and Zhang, Q.: Trends in China's
1168 anthropogenic emissions since 2010 as the consequence of clean air actions,
1169 Atmos. Chem. Phys., 18, 14095–14111,
1170 <https://doi.org/10.5194/acp-18-14095-2018>, 2018.
- 1171 Zheng, B., Cheng, J., Geng, G., Wang, X., Li, M., Shi, Q., Qi, J., Lei, Y., Zhang, Q.,
1172 and He, K.: Mapping anthropogenic emissions in China at 1 km spatial
1173 resolution and its application in air quality modeling, Sci. Bull., 66, 612-620,
1174 <https://doi.org/10.1016/j.scib.2020.12.008>, 2021.
- 1175 Zheng, J., Zhang, L., Che, W., Zheng, Z., and Yin, S.: A highly resolved temporal and
1176 spatial air pollutant emission inventory for the Pearl River Delta region, China
1177 and its uncertainty assessment, Atmos. Environ., 43, 5112-5122,
1178 [10.1016/j.atmosenv.2009.04.060](https://doi.org/10.1016/j.atmosenv.2009.04.060), 2009.
- 1179 Zheng, J. J., Jiang, P., Qiao, W., Zhu, Y., and Kennedy, E.: Analysis of air pollution
1180 reduction and climate change mitigation in the industry sector of Yangtze River



1181 Delta in China, J. Clean. Prod., 114, 314–322,
1182 <https://doi.org/10.1016/j.jclepro.2015.07.011>, 2016.
1183 Zhou, Y., Zhao, Y., Mao, P., Zhang, Q., Zhang, J., Qiu, L., and Yang, Y.: Development
1184 of a high-resolution emission inventory and its evaluation and application
1185 through air quality modeling for Jiangsu Province, China, Atmos. Chem. Phys.,
1186 17, 211–233, <https://doi.org/10.5194/acp-17-211-2017>, 2017.
1187



1188 **Figure captions**

1189 Figure 1. Emission trends, underlying social and economic factors. Coal consumption
1190 is achieved by Chinese Energy Statistics (National Bureau of Statistics, 2016-2020).
1191 The GDP, population, and vehicle population data come from the National Bureau of
1192 Statistics, (2016-2020). Data are normalized by dividing the value of each year by
1193 their corresponding value in 2015.

1194 Figure 2. Anthropogenic emissions by sector and year. The species include (a) SO₂, (b)
1195 NO_x, (c) CO, (d) AVOCs, (e) NH₃, (f) PM₁₀, (g) PM_{2.5}, (h) BC, and (i) OC. Emissions
1196 are divided into five sectors: power, industry, transportation, residential, and
1197 agriculture.

1198 Figure 3. Changes in emissions by sector and year. The species include (a) SO₂, (b)
1199 NO_x, (c) CO, (d) AVOCs, (e) NH₃, (f) PM₁₀, (g) PM_{2.5}, (h) BC, and (i) OC. The 2015
1200 emissions are subtracted from the emission data for each year to represent the
1201 additional emissions compared to 2015 levels.

1202 Figure 4. The city-level emissions and spatial distribution include (a) SO₂, (b) NO_x, (c)
1203 AVOCs, (d) PM_{2.5}, and (e) NH₃; and (f) the proportions of emission by different
1204 regions for 2015 and 2019. The blue line indicates the Yangtze River. The map data
1205 provided by Resource and Environment Data Cloud Platform are freely available for
1206 academic use (<http://www.resdc.cn/data.aspx?DATAID=201>), © Institute of
1207 Geographic Sciences & Natural Resources Research, Chinese Academy of Sciences.

1208 Figure 5. Difference in the spatial distribution of major pollutant emissions between
1209 2015 and 2019 for (a) SO₂, (b) NO_x, (c) PM_{2.5}, and (d) AVOCs. The black circles
1210 represent the locations of top 10 emitters for corresponding species in each panel. The
1211 blue line indicates the Yangtze River.

1212 Figure 6. The ratios of BVOCs to AVOCs emissions in July: (a) 2015, (b) 2017, and (c)
1213 2019.

1214 Figure 7. Comparison of interannual trends with MEIC, EDGAR, and ground-based
1215 observations: (a) SO₂ and (b) NO_x (NO₂).



1216 Figure 8. Comparison of Jiangsu emissions for 2017 with MEIC and An et al. (2021).
1217 The air pollutants from left to right are SO₂, NO_x, VOCs, NH₃, and PM_{2.5},
1218 respectively.

1219 Figure 9. Contributions of individual measures to emission reductions in SO₂, NO_x,
1220 VOCs, and PM_{2.5} for 2015-2017 (the left column) and 2017-2019 (the right column).

1221 Figure 10. The monthly averages of (a) PM_{2.5} and (b) MDA8 O₃ from CMAQ
1222 simulation and ground observation for January, April, July and October from 2015 to
1223 2019. The slopes of linear regressions in the panels indicate the annual variation rates
1224 for corresponding species.

1225 Figure 11. The concentration changes during 2015-2017 and 2017-2019 from CMAQ
1226 for (a) PM_{2.5} and (b) O₃ (VEMIS and VMET: meteorological conditions and
1227 emissions fixed at 2017 level, respectively).

1228



1229 **Tables**

1230 **Table 1 Annual emissions of BVOCs and AVOCs and the ratios of BVOCs to**
1231 **AVOCs.**

	Year	January	April	July	October	Annual
BVOCs (Gg)	2015	0.0020	8.1	38.0	3.9	150.0
	2016	0.0017	8.5	51.4	2.8	188.1
	2017	0.0023	9.4	58.7	2.8	212.7
	2018	0.0020	9.1	55.5	3.5	204.3
	2019	0.0017	6.9	53.4	4.1	193.2
AVOCs (Gg)	2015	131.3	102.8	101.8	104.0	1348.3
	2016	131.2	102.3	101.3	103.6	1346.4
	2017	123.4	97.0	96.0	98.2	1342.9
	2018	131.6	102.5	101.6	103.8	1306.0
	2019	127.7	99.4	98.4	100.6	1271.1
BVOCs/AVOCs (%)	2015	0.0	7.9	37.3	3.8	11.1
	2016	0.0	8.3	50.7	2.7	14.0
	2017	0.0	9.7	61.2	2.9	15.8
	2018	0.0	8.9	54.6	3.4	15.6
	2019	0.0	6.9	54.3	4.1	15.2

1232

1233

1234

1235

1236

1237

1238

1239

1240

1241

1242

1243



1244 **Table 2 Air pollutant emissions in Jiangsu and comparison with previous studies**

	Data source	Annual air pollutant emissions (Gg·yr ⁻¹)						
		SO ₂	NO _x	AVOCs	NH ₃	CO	PM ₁₀	PM _{2.5}
2014	Li et al. (2018)	1002	1315	1560	544	12667	1761	779
2015	This study	627	1411	1348	468	7735	711	491
	MEIC	626	1646	2143	544	9059	595	444
	REAS	649	1343	2063	611	10980	827	622
	Sun et al. (2018)	1230	1700	2000		13780		
	Zhang et al. (2017)				703			
2016	This study	580	1391	1346	452	7397	687	475
	MEIC	468	1586	2128	532	8191	516	388
	Simayi et al. (2019)			2024				
2017	This study	416	1331	1343	434	7305	676	468
	MEIC	315	1538	2132	528	7731	492	367
	An et al. (2021)	619	1165	2056	1093	17309	1440	404
2018	This study	374	1198	1306	430	7252	670	462
	MEIC	336	1456	1999	484	6513	365	272
	Gao et al. (2022)	210	830	3000	530	9950	310	260
2019	This study	296	1122	1271	422	7163	565	411
	MEIC	311	1414	1983	455	6380	351	263

1245

1246

1247

1248

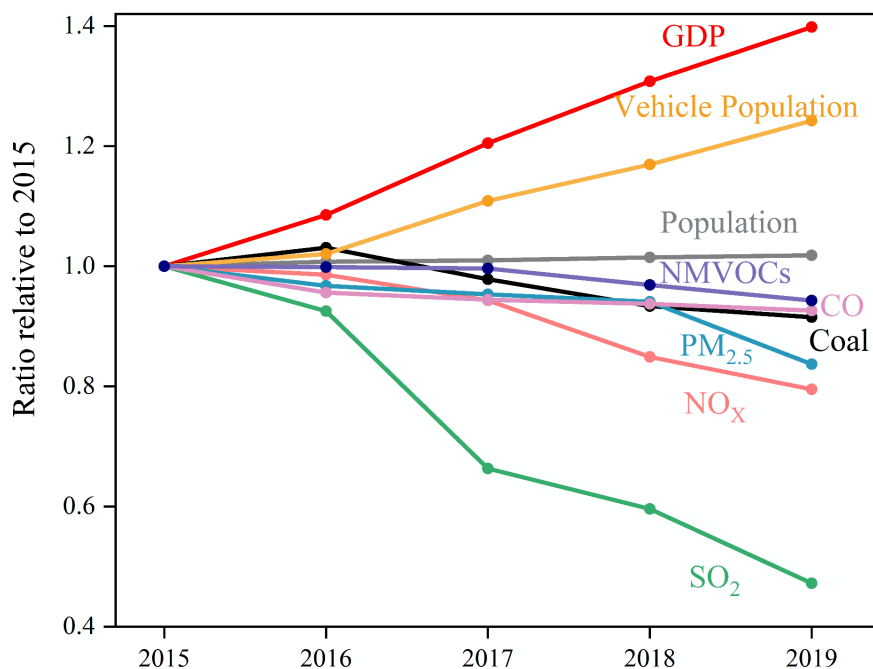
1249

1250

1251



1252 **Figure 1**

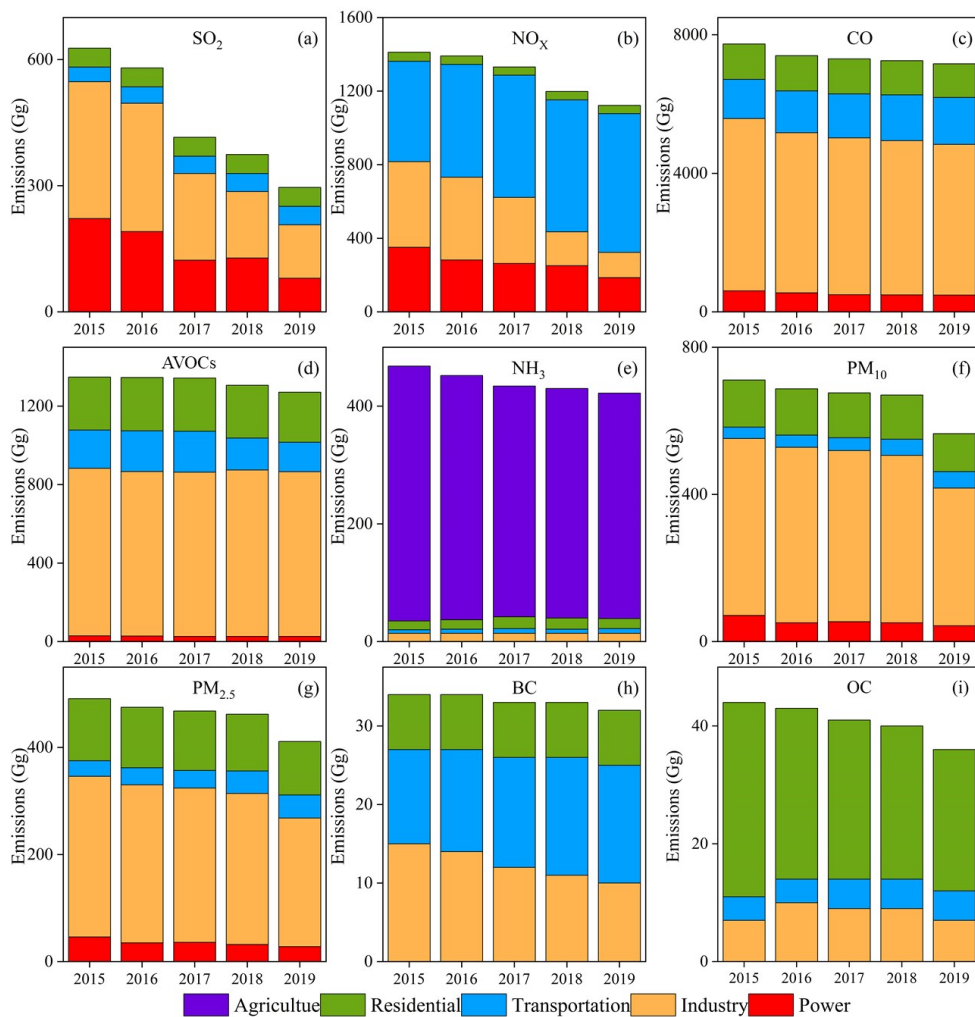


1253
1254
1255
1256
1257
1258
1259
1260
1261
1262
1263
1264
1265
1266



1267 **Figure 2**

1268



1269

1270

1271

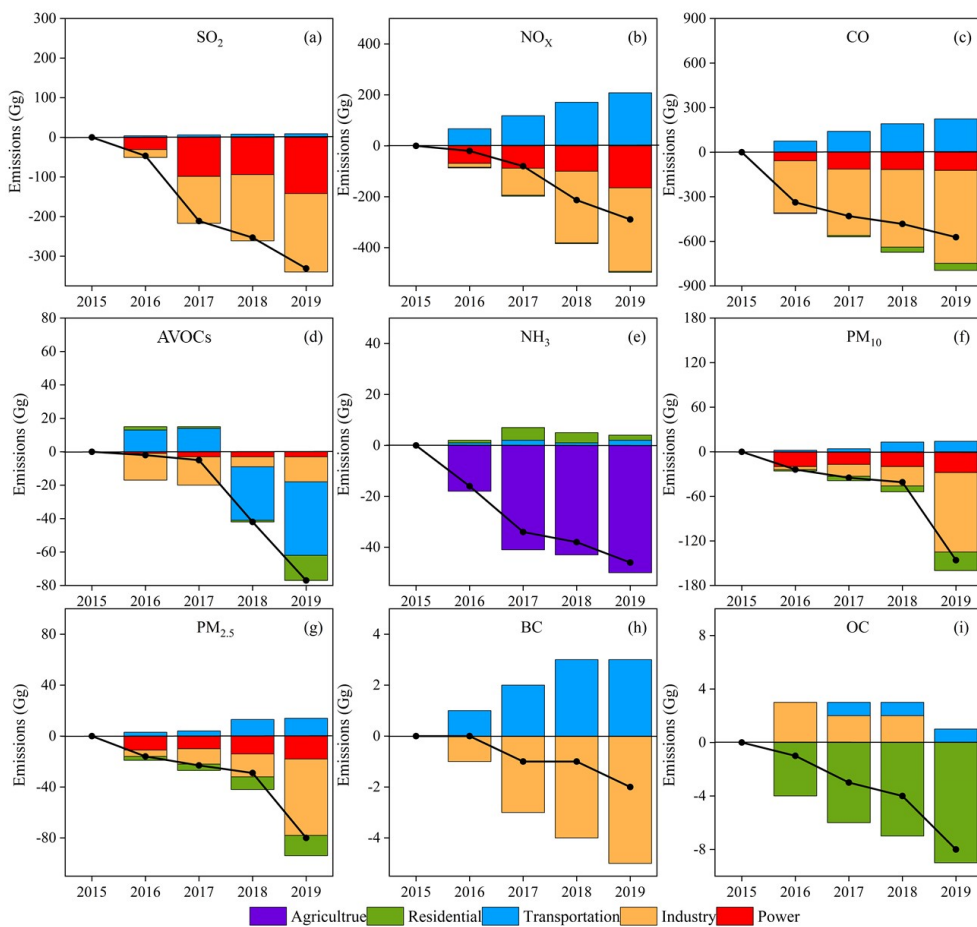
1272

1273

1274



1275 **Figure 3**



1276

1277

1278

1279

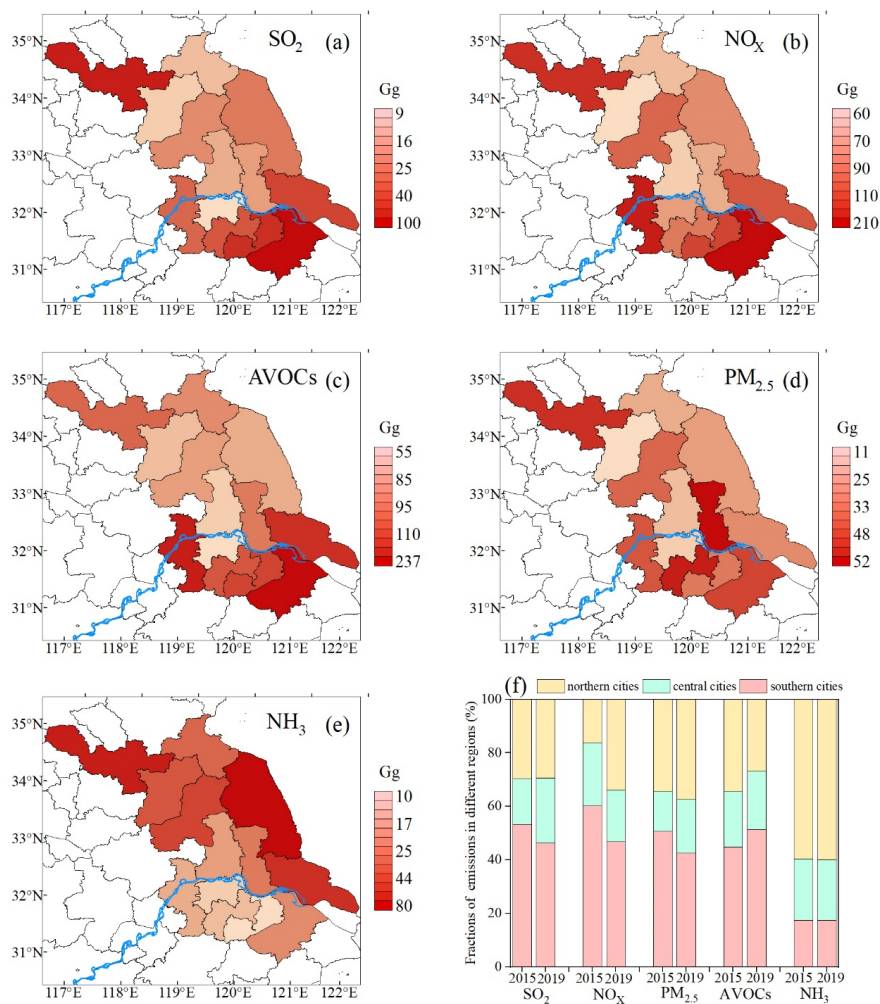
1280

1281

1282



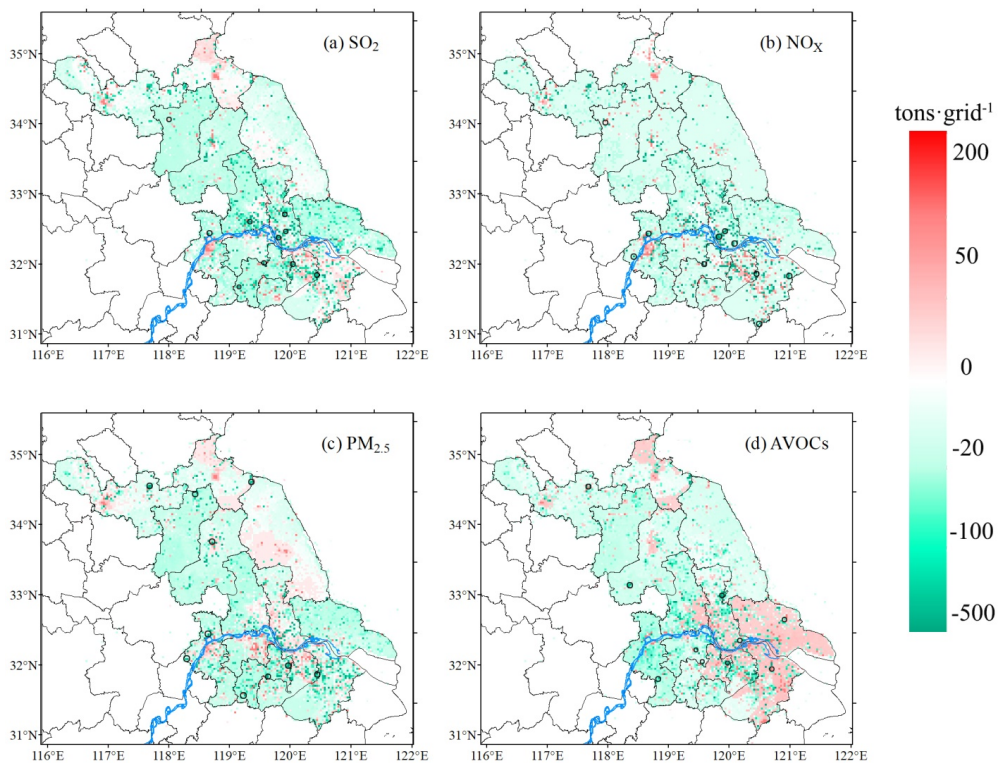
1283 **Figure 4**



1284



1285 **Figure 5**

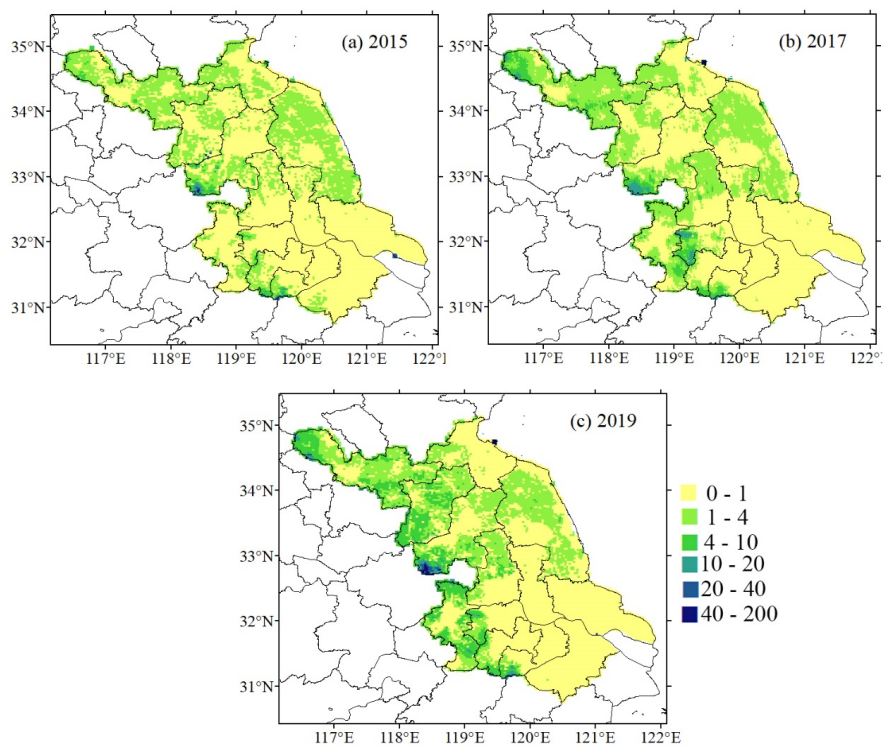


1286

1287



1288 **Figure 6**



1289

1290

1291

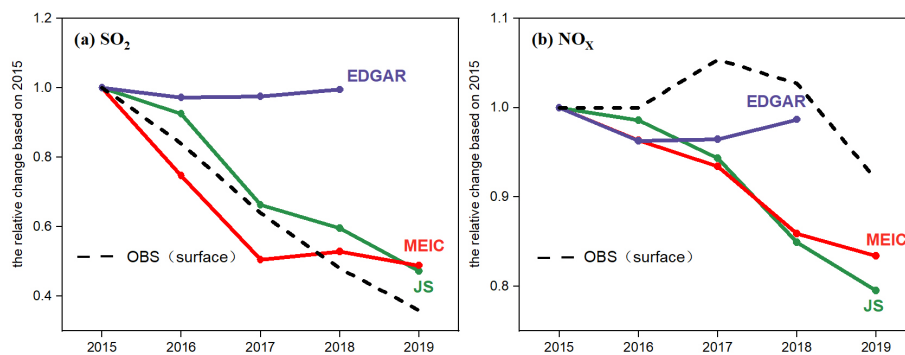
1292

1293

1294



1295 **Figure 7**



1296

1297

1298

1299

1300

1301

1302

1303

1304

1305

1306

1307

1308

1309

1310

1311

1312

1313

1314

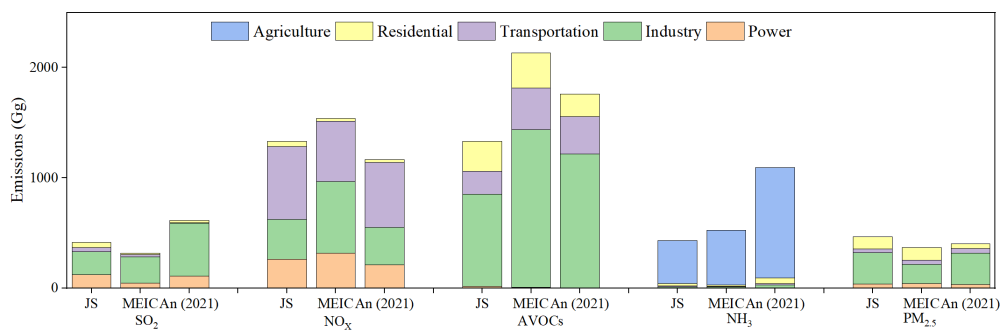
1315

1316

1317



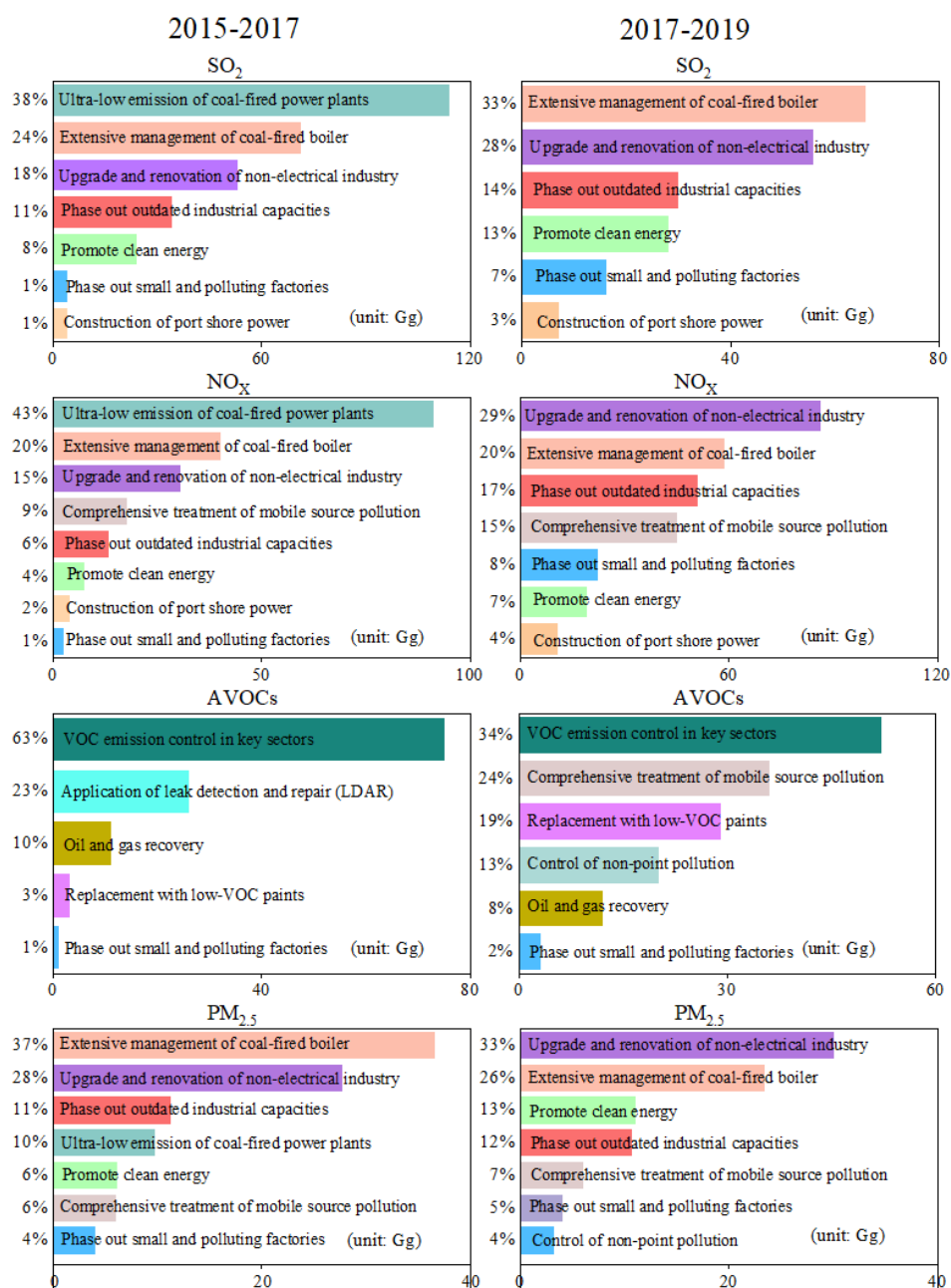
1318 **Figure 8**



1319
1320
1321
1322
1323
1324
1325

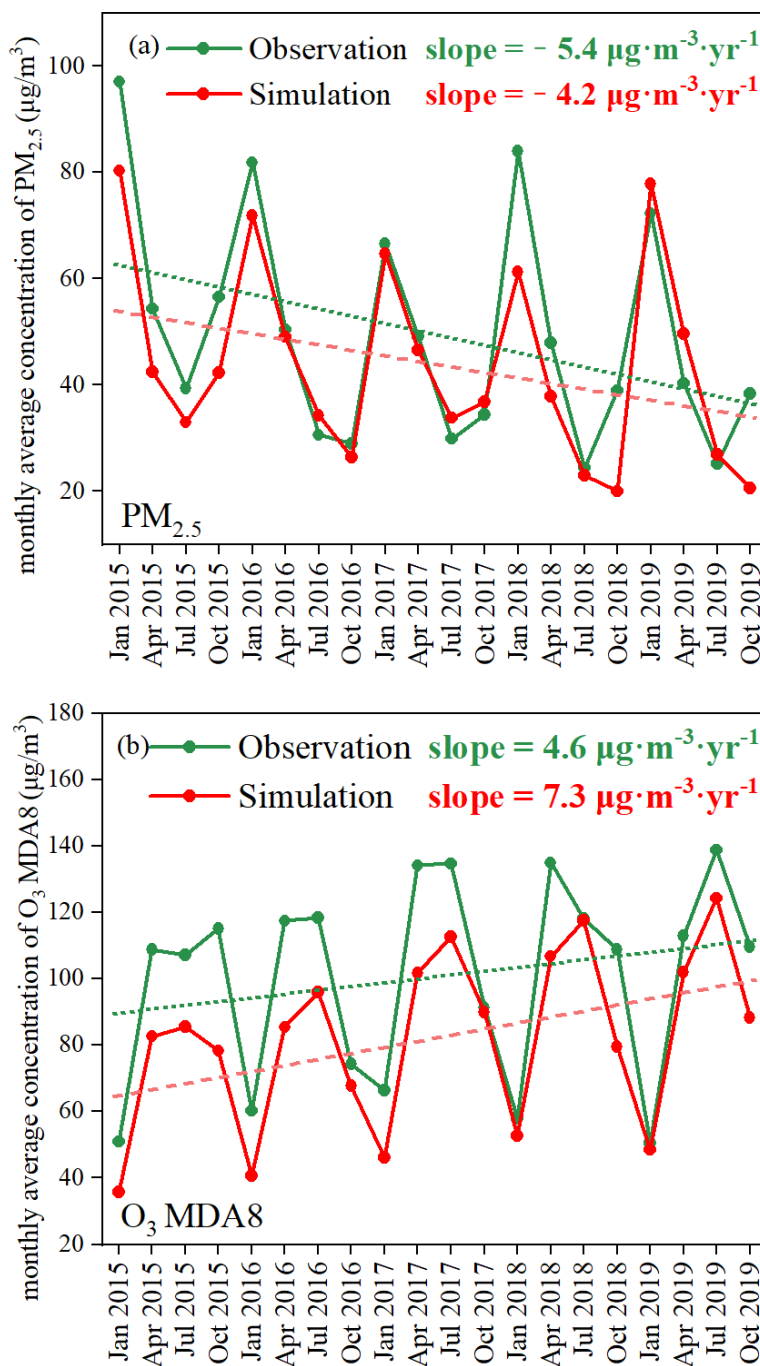


1326 **Figure 9**





1328 **Figure 10**



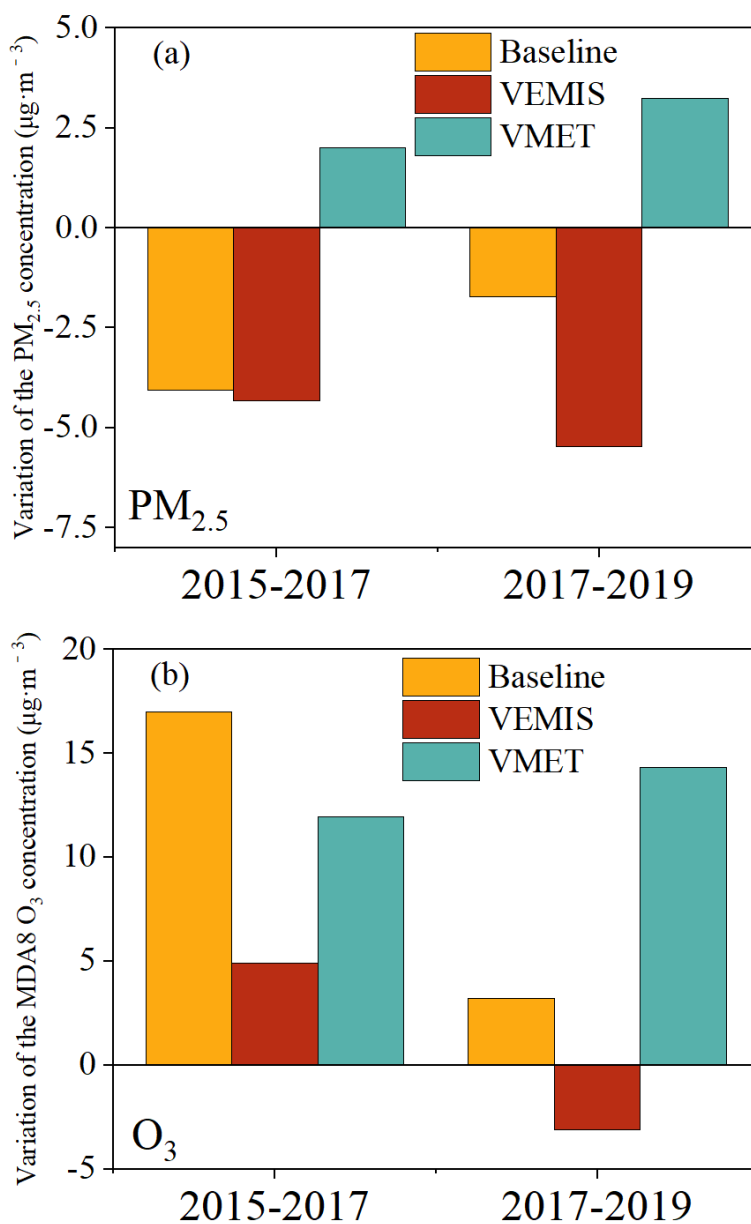
1329

1330



1331

1332 **Figure 11**



1333

1334